A Schumann Resonance-based Quantity for Characterizing Day-to-day Changes in Global Lightning Activity

Tamas Bozoki[1], Gabriella Sátori[2], Earle Williams[3], Anirban Guha[4], Yakun Liu[3], Peter Steinbach[5], ADÔNIS FERREIRA RAIOL LEAL[6], Mike Atkinson[7], Ciaran D Beggan[8], Elizabeth DiGangi[9], Alexander V Koloskov[10], Andrzej Kulak[11], Jeff Lapierre[12], David K. Milling[13], Janusz Mlynarczyk[11], Anne Neska[14], Alexander S. Potapov[15], Tero Raita[16], Rahul Rawat[17], Ryan K Said[18], Ashwini Kumar Sinha[17], and Yuri M Yampolski[19]

[1]Institute of Earth Physics and Space Science (ELKH EPSS)
[2]Geodetic and Geophysical Research Insitute, Hungarian Academy of Sciences
[3]Massachusetts Institute of Technology
[4]Tripura University
[5]Eötvös Loránd Research Network (ELKH)
[6]Federal University of Para
[7]HeartMath Institute
[8]British Geological Survey
[9]Earth Networks Inc.
[10]Institute of Radio Astronomy
[11]AGH University of Science and Technology
[12]Advanced Environmental Monitoring (AEM)
[13]University of Alberta
[14]Institute of Geophysics, Polish Academy of Sciences
[15]ISTP SB RAS
[16]Sodankylä Geophysical Observatory, University of Oulu
[17]Indian Institute of Geomagnetism
[18]Vaisala, Inc.
[19]Institute of Radio Astronomy, Ukraine

January 24, 2023

Abstract

The importance of lightning has long been recognized from the point of view of climate-related phenomena. However, the detailed investigation of lightning on global scales is currently hindered by the incomplete and spatially uneven detection efficiency of ground-based global lightning detection networks and by the restricted spatio-temporal coverage of satellite observations. We are developing different methods for investigating global lightning activity based on Schumann resonance (SR) measurements. SRs are global electromagnetic resonances of the Earth-ionosphere cavity maintained by the vertical component of lightning. Since charge separation in thunderstorms is gravity-driven, charge is typically separated vertically in thunderclouds, so every lightning flash contributes to the measured SR field. This circumstance makes SR measurements very suitable for climate-related investigations. In this study, 19 days of global lightning activity in January 2019 are analyzed based on SR intensity records from 18 SR stations and the results are compared with independent lightning observations provided by ground-based (WWLLN, GLD360 and ENTLN) and satellite-based (GLM, LIS/OTD) global lightning detection. Daily average SR intensity records from different stations exhibit strong similarity in the investigated time interval. The inferred intensity of global lightning activity varies by a factor of 2-3 on the time scale of 3-5 days which we attribute to continental-scale temperature changes related to cold air outbreaks from polar regions. While our results demonstrate that the SR phenomenon is a powerful tool to investigate global lightning, it is also clear that currently available technology limits the detailed quantitative evaluation of lightning activity on continental scales.

A Schumann Resonance-based Quantity for Characterizing Day-to-day Changes in Global Lightning Activity

T. Bozóki[1,2], G. Sátori[1], E. Williams[3], A. Guha[4], Y. Liu[3], P. Steinbach[5,6], A. Leal[7,8], M. Atkinson[9], C. D. Beggan[10], E. DiGangi[11], A. Koloskov[12,13], A. Kulak[14], J. LaPierre[11], D.K. Milling[15], J. Mlynarczyk[14], A. Neska[16], A. Potapov[17], T. Raita[18], R. Rawat[19], R. Said[20], A.K. Sinha[21], Y. Yampolski[22]

[1]Institute of Earth Physics and Space Science (EPSS), Sopron, Hungary.

[2]Department of Optics and Quantum Electronics, University of Szeged, Szeged, Hungary.

[3]Parsons Laboratory, Massachusetts Institute of Technology, Cambridge, Massachusetts, USA.

[4]Department of Physics, Tripura University, Agartala, India.

[5]Department of Geophysics and Space Science, Eötvös Loránd University, Budapest, Hungary.

[6]ELKH-ELTE Space Research Group, Budapest, Hungary.

[7]Department of Physics and Langmuir Laboratory, New Mexico Institute of Mining and Technology, Socorro, NM, USA.

[8]Graduate Program in Electrical Engineering, Federal University of Pará, Belem, Brazil.

[9]HeartMath Institute, Boulder Creek, CA, USA.

[10]British Geological Survey, Edinburgh, UK.

[11]Advanced Environmental Monitoring (AEM), Maryland, USA.

[12]Department of Physics, University of New Brunswick, Fredericton, NB, Canada.

[13]State Institution National Antarctic Scientific Center of Ukraine, Kyiv, Ukraine.

[14]Institute of Electronics, AGH University of Science and Technology, Krakow, Poland.

[15]Department of Physics, University of Alberta, Edmonton, Canada.

[16]Institute of Geophysics, Polish Academy of Sciences, Warsaw, Poland.

[17]Institute of Solar-Terrestrial Physics SB RAS, Irkutsk, Russia.

[18]Sodankylä Geophysical Observatory, University of Oulu, Sodankylä, Finland.

[19]Indian Institute of Geomagnetism, Navi Mumbai, India.

[20]Vaisala, Louisville, CO, USA.

[21]Department of Physics, School of Science, University of Bahrain, Bahrain.

[22]Institute of Radio Astronomy, National Academy of Sciences of Ukraine, Kharkiv, Ukraine.

Corresponding author: Tamás Bozóki (Bozoki.Tamas@epss.hu)

Key Points

- Daily average SR intensity is a quasi-global invariant quantity that shows good agreement with global daily stroke rates and thunder hours.
- Global lightning activity can vary by a factor of 2-3 on a 3-5 day timescale which could be attributed to cold air outbreaks.
- Currently available technology does not allow the detailed quantitative evaluation of lightning activity on continental scales.

Abstract

The importance of lightning has long been recognized from the point of view of climate-related phenomena. However, the detailed investigation of lightning on global scales is currently hindered by the incomplete and spatially uneven detection efficiency of ground-based global lightning detection networks and by the restricted spatio-temporal coverage of satellite observations. We are developing different methods for investigating global lightning activity based on Schumann resonance (SR) measurements. SRs are global electromagnetic resonances of the Earth-ionosphere cavity maintained by the vertical component of lightning. Since charge separation in thunderstorms is gravity-driven, charge is typically separated vertically in thunderclouds, so every lightning flash contributes to the measured SR field. This circumstance makes SR measurements very suitable for climate-related investigations. In this study, 19 days of global lightning activity in January 2019 are analyzed based on SR intensity records from 18 SR stations and the results are compared with independent lightning observations provided by ground-based (WWLLN, GLD360 and ENTLN) and satellite-based (GLM, LIS/OTD) global lightning detection. Daily average SR intensity records from different stations exhibit strong similarity in the investigated time interval. The inferred intensity of global lightning activity varies by a factor of 2-3 on the time scale of 3-5 days which we attribute to continental-scale temperature changes related to cold air outbreaks from polar regions. While our results demonstrate that the SR phenomenon is a powerful tool to investigate global lightning, it is also clear that currently available technology limits the detailed quantitative evaluation of lightning activity on continental scales.

Plain Language Summary

Lightning is recognized as a climate variable indicating the changing climate of the Earth. Surface temperature changes on the order of 1 ^{o}C can result in a significant change in lightning frequency. Lightning activity is monitored on a global scale by satellites and by ground-based global lightning detection networks. However, the detection efficiency of these available technologies is limited which restricts the investigation of global lightning activity especially on the day-to-day time scale. In this study, we propose an alternative method to monitor day-to-day changes in global lightning activity based on Schumann resonance (SR) measurements and thus we compare SR-based observations with available global lightning monitoring techniques. We show that the overall intensity of global lightning activity can vary considerably (by a factor of 2-3) within a few days, further motivating our efforts to monitor

such changes. It is also clear from our study that new methods are needed to quantitatively characterize continental-scale lightning activity.

1. Introduction

Global lightning activity is known as an essential indicator of global climate and has the potential to reveal important consequences of climate change (Aich et al., 2018). The main argument behind this statement is the nonlinear relation between lightning activity and surface temperature (Williams, 1992). Temperature perturbations on the order of 1 °C have pronounced local effects on cloud electrification which can result in a significant change in lightning frequency (up to 10% per 1 °C) depending on the time scale investigated (Williams, 2005). A dramatic increase (up to 300%) of lightning has been revealed at Arctic latitudes which correlates well with the global temperature anomaly indicating a temperature enhancement from 0.65°C to 0.95°C in the Arctic region (Holzworth et al., 2021). However, there is some uncertainty in this result, which is related to the time-dependent detection efficiency of the applied lightning detection network. In a more global context it has been shown that the global lightning record from the Lightning Imaging Sensor (LIS) shows statistically flat behavior over the 2002–2013 period, which is often termed a 'hiatus' in global warming with flat temperature trend (Williams et al., 2019). Recently, the radiated energy of global lightning activity has been described using a rigorous quantum physics framework, which is expected to help better understand the impact of climate change on global lightning and the Earth's atmosphere in general (Füllekrug, 2021a).

Lightning is not only an indicator but also a driver of climate change by producing strong greenhouse gasses (Price et al., 1997; Schumann & Huntrieser, 2007). A strong correlation has also been found between convective intensity and upper tropospheric water vapor, one further key element of Earth's climate, and lightning is related to convective intensity (Plotnik et al., 2021; Price, 2000). This result underlines that thunderstorms play an important role in the global redistribution of water, a key mediator of both short and long wavelength radiation (Williams, 2005). All these aspects motivate efforts to monitor the long-term characteristics of lightning on local, regional, and global scales, including the stroke occurrence rate, the average charge transfer, the flash intensity and extent, as well as the distribution of thunderstorm-affected areas, lightning hotspots and lightning superbolts (e.g., Albrecht et al., 2016; Beirle et al., 2014; Blakeslee et al., 2014; Blakeslee et al., 2020; Boldi et al., 2018; Cecil et al., 2015; Chronis & Koshak, 2017; Holzworth et al., 2019; Lyons et al., 2020; Peterson et al., 2021).

About 50 lightning flashes occur every second at any given time on Earth (Christian et al., 2003) and this rate can vary by as much as 10-20% on different time scales (Aich et al., 2018; Albrecht et al., 2016; Cecil et al., 2014; Williams, 2020). Optical detection carried out by satellites provides one way to study lightning activity on global scales. Lightning detection from Low Earth Orbit (LEO), like the Lightning Imaging Sensor (LIS) onboard the Tropical Rainfall Measuring Mission (TRMM, 1997-2015, Christian et al., 2003) and the International Space Station (ISS, February 2017-present, Blakeslee et al., 2020), lays the foundations for essential statistical studies. The limitation of this technique is that continuous monitoring of a specific thunderstorm area is not possible as lightning strokes outside the suborbital swath are not detected. On the other hand, lightning detection from Geostationary Earth Orbit (GEO), like the Geostationary Lightning Mapper (GLM) instrument onboard the GOES-R series satellites (Goodman et al., 2013) and the Lightning Mapping Imager (LMI) instrument onboard the FengYun-4A satellite (Yang et al., 2017), provides continuous lightning monitoring for a given longitudinal sector. Although the appearance of these satellite-based methods represent a major advance for lightning detection on global scales, the current lack of global coverage (i.e., all longitudinal sectors) and the general limitations of optical lightning detection (e.g., the dependence on cloud thickness and time of the day) call for alternative approaches.

Ground-based monitoring of global lightning activity represents another possibility for lightning research, with simultaneous world-wide coverage and with less elaborate and costly infrastructure. Global ground-based lightning monitoring utilizes the electromagnetic (EM) signal emitted by lightning for detection. As the power radiated by lightning peaks in the Very Low Frequency (VLF, 3–30 kHz) band (Wait, 1970) global lightning activity can be monitored with a network of VLF receivers. Such networks require hundreds of VLF (or broadband) receiver stations to achieve global coverage. The World Wide Lightning Location Network (http://wwlln.net) is a collaboration among over 50 universities and institutions for providing lightning locations based on this technique. Currently, two additional global lightning detection networks are in operation: the Global Lightning Detection Network (GLD360) of Vaisala and Earth Networks Total Lightning Network (ENTLN).

The detection efficiency of global lightning detection networks is a key issue for their applicability in climate research (Virts et al., 2013). However, the detection efficiencies are generally unknown, partly because of the lack of a reliable reference dataset (Burgesser, 2017) and partly because of the confidentiality of this information for commercially-operated networks. Even the locations of receiver stations are known only for the research-oriented WWLLN network. For a one year period between November 2014 and October 2015, the absolute global detection efficiency of GLD360, ENTLN and WWLLN has been estimated to be 59.8%, 56.8% and 7.9%, respectively, based on Bayesian analysis (Bitzer & Burchfield, 2016). However, for relatively strong discharges these values are significantly higher (for example in the case of the WWLLN this detection efficiency is about 50% based on Hutchins et al., 2012). It is to be emphasized that these detection efficiencies are spatially uneven (see e.g., Hutchins et al., 2012; Marchand et al., 2019; Rudlosky et al., 2015), restricts detailed investigation of lightning on global scales and prevents the detailed quantitative comparison of lightning activity on continental scales on time scales ranging from the diurnal to the interannual. One important example of this limitation is that lightning activity in Africa is usually underestimated by these networks as compared to Earth's other two main lightning 'chimneys' in the Americas and Asia (Williams & Mareev, 2014). The lower number of receiver stations in the African region is one of the plausible explanations for this observation (Williams & Mareev, 2014). From all these aspects it can be concluded that despite substantial interest in investigating global lightning activity for meteorological/climatological purposes, this endeavor is considerably limited by the vagaries of detection efficiency with available lightning monitoring technologies.

The attenuation of EM waves in the lowest part (<100 Hz) of the Extremely Low Frequency (ELF, 3 Hz - 3 kHz) band (in the range of 0.2-0.5 dB/Mm; Chapman et al., 1966; Wait, 1970) is substantially smaller than in the VLF band (in the range of 1-10 dB/Mm; Barr et al., 2000; Hutchins et al., 2013; Taylor, 1960). This fact enables the investigation of global lightning activity with a much lower number of receiver stations (1–20). In the ELF band lightning-radiated EM waves travel a number of times around the globe in the waveguide formed by the Earth's surface and the lower ionosphere before losing most of their energy. The constructive interference of the EM waves propagating in opposite directions (direct and antipodal waves) creates global EM resonances called Schumann resonances (SRs) which can be observed at ~8, ~14, ~20, etc. Hz (Balser & Wagner, 1960; Galejs, 1972; Madden & Thompson, 1965; Nickolaenko & Hayakawa, 2002; Price, 2016; Schumann, 1952; Wait, 1970). While SR frequencies can be used to deduce temporal changes in the global displacement and migration of lightning activity (e.g., Koloskov et al., 2020; Sátori, 1996; Sátori & Zieger, 1999; Sátori & Zieger, 2003) as well as in the areal compactness of global lightning (Nickolaenko & Rabinowicz, 1995; Nickolaenko et al., 1998; Sátori & Zieger, 2003), SR intensities are known to indicate the overall intensity of global lightning activity (Boldi et al., 2018; Clayton & Polk, 1977; Heckman et al., 1998; Nickolaenko & Hayakawa, 2002; Sentman & Fraser, 1991). Several works have already shown that variations of SRs are consistent with climatological lightning distributions provided by satellite-based lightning detection (e.g., Boldi et al., 2018; Füllekrug, 2021b; Sátori et al., 2009). SRs represent the transverse magnetic (TM) resonance mode of the Earth-ionosphere cavity resonator, which can be excited by vertical lightning discharges (Jackson, 1975). Since the ice-based process of charge separation in thunderstorms is gravity-driven, charge is basically separated vertically in a thundercloud, so every lightning flash in the atmosphere (intracloud and cloud-to-ground alike) is guaranteed to contribute to the SR intensity. This makes SR observations well-suited for climate-related studies (see e.g., Sátori, 1996; Sátori et al., 2009; Williams, 2020; Williams et al., 2021).

The AC global electric circuit as manifest in Schumann resonances is a technically-involved electromagnetic phenomenon (Madden & Thompson, 1965), standing in sharp contrast with the simpler treatment of the DC global electric circuit, which is modeled as a giant spherical capacitor (Haldoupis et al., 2017) characterized by a single scalar: the ionospheric potential (Markson, 2007). The long-standing quest for an equivalent scalar quantity for SRs was initiated by Sentman & Fraser (1991) as the sum of magnetic modal intensities. The aim here was to average out the complicated source-receiver distance effects to approximate the global behavior by introducing a globally invariant SR-based quantity. Their three-decade-old suggestion is tested in the present work in an unprecedented way.

The understanding of the response of global lightning to temperature on short time scales has been stymied historically by the traditional monthly resolution of datasets on global surface air temperature (e.g., Hansen & Lebedeff, 1987). In this study, the global land surface temperature anomaly and lightning activity are analyzed with daily resolution. This investigation has the potential to reveal important variability of the climate system that could change over time as a result of climate change. On this time scale, global effects of cold air outbreaks, when very cold air masses are transported from polar to mid- and low-latitudes, become readily apparent, as will be elaborated on below.

Episodic intrusions of cold air from high latitudes into warmer air at low latitudes have been extensively investigated under the names 'cold surges', 'polar air outbreaks', 'cold air outbreaks' and 'freeze events', and provide a plausible explanation for global temperature perturbations lasting for one to several days. In extreme events, the colder equator-moving air can extend across the equator into the opposite hemisphere and impact the local tropical temperature at the level of 1C. An excellent summary can be found in Hastenrath (1996). Such events may originate in either northern (Hartjenstein & Block, 1991) or southern hemispheres, but the literature is more abundant in studies in southern hemisphere winter (Kousky, 1979; Lanfredi & Camargo, 2018; Lupo et al., 2001; Marengo et al., 1997; Prince & Evans, 2018). The reason for this imbalanced attention may arise because the Antarctic winter air is colder than Arctic air, and because the protection of coffee plantations during freeze events in Brazil is of substantial economic interest (Marengo et al., 1997). The longitudinally-confined nature of the polar outbreaks results in lower-latitude impacts that are sometimes confined to individual continental chimneys (America, Africa, Southeast Asia), with corresponding collections of events in Prince & Evans (2018), Crossett & Metz (2017), Murakami (1979), respectively, or to broader impacts affecting multiple chimneys (Metz et al., 2013) as the equatorward-moving cold air also advects eastward.

In this study, we analyze global lightning activity from 13 to 31 January 2019 based on SR intensity records from 18 SR stations around the globe and compare the results with lightning observations provided by independent ground-based (WWLLN, GLD360 and ENTLN) and satellite-based (GLM, LIS/OTD) global lightning detection. The main motivation of this study is a) to show that global lightning can vary substantially on a day-to-day basis and b) to demonstrate that SR measurements are very well suited to monitor and investigate these day-to-day variations. It is to be highlighted that this is the first study to analyze such a large number of SR stations simultaneously. We will show that summing the first three modes of the two magnetic field components and averaging these values on a daily basis results in a quantity that exhibits very similar (but not exactly identical) behavior at all SR stations studied, and is therefore called a quasi-global invariant.

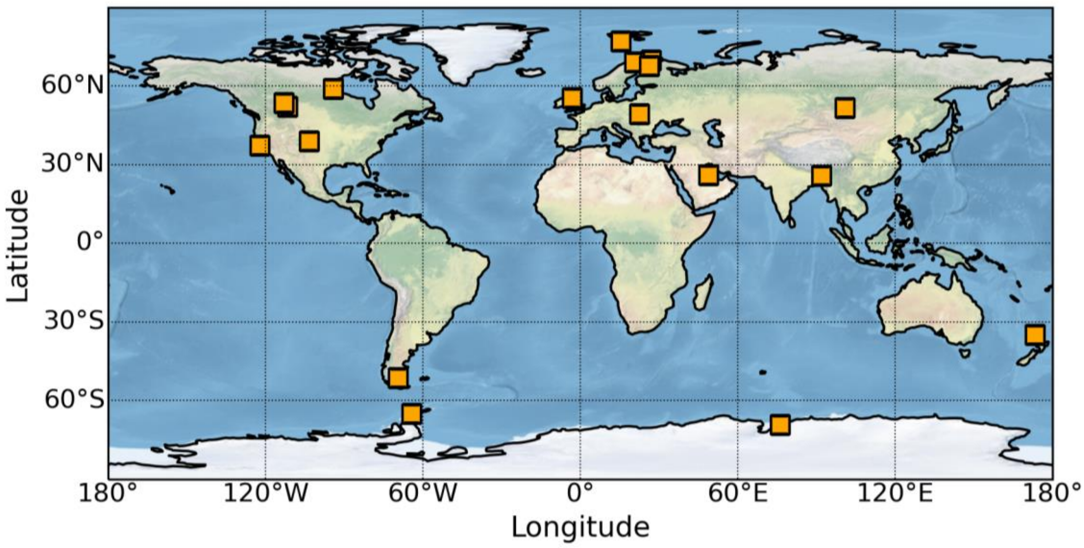

Figure 1. Map showing the locations of the 18 SR stations used in the study (marked by orange squares).

2. Data and Methods

2.1. Data on Schumann Resonances

The most important information about the 18 SR stations used in this study are listed in Table 1 and their locations are shown in Fig.1. All the stations are equipped with a pair of induction coil magnetometers that are in most cases aligned with the local geographical meridian and perpendicular to it, except at the Fort Churchill (FCHU), Ministik Lake (MSTK) and Mondy (MND) stations where they are oriented along the geomagnetic north-south (NS) and east-west (EW) directions. The ALB, BOU, HOF and NOR stations are operated by the Heartmath Institute (https://www.heartmath.org/gci/) and are used mainly to study the relationship between humans and our electromagnetic environment (e.g., Timofejeva et al., 2021). The BRT and SHI stations are operated by the Indian Institute of Geomagnetism. The low resolution (64 Hz) data from the low latitude SHI station in India have been used to study ionospheric Alfven resonances (IAR) (e.g., Adhitya et al., 2022) while high resolution (256 Hz) data from the Antarctic BRT station have been used to examine finer structures of electromagnetic ion cyclotron (EMIC) waves (e.g., Kakad et al., 2018; Upadhyay et al., 2022). The ESK station is operated by the British Geological Survey and is dedicated to study SRs and ionospheric Alfven resonances (see e.g., Beggan & Musur, 2018; Musur & Beggan, 2019). The HRN station in Svalbard is maintained by the Institute of Geophysics (Polish Academy of Sciences) and has been used to study SRs for almost two decades (e.g., Neska et al., 2019; Sátori et al., 2007). The MND station belongs to the Institute of Solar-Terrestrial Physics (Russian Academy of Sciences). This station has been recently used to investigate globally observable ELF-transients (Marchuk et al., 2022). The VRN station in Antarctica is operated by the Institute of Radio Astronomy (National Academy of Sciences of Ukraine) and is one of the most extensively used stations in SR research (e.g., Koloskov et al., 2020; Koloskov et al., 2022; Sátori et al., 2016). The FCHU and MSTK stations are part of the CARISMA network (carisma.ca, Mann et al., 2008) operated by the University of Alberta. These stations are mainly used to study EMIC/Pc1 waves (Kim et al., 2018; Matsuda et al., 2021). The HUG, HYL and PAT stations belong to the World ELF Radiolocation Array (WERA, http://www.oa.uj.edu.pl/elf/index/projects3.htm, Kulak et al., 2014) operated by the Krakow ELF group. The primary objective of WERA is to radiolocate and characterize strong lightning discharges from around the world (e.g., Marchenko et al., 2020; Mlynarczyk et al., 2017; Strumlik et al., 2021). The KEV, KIL and SOD stations are part of the Finnish pulsation magnetometer chain (https://www.sgo.fi/Data/Pulsation/pulDescr.php) operated by the Sodankylä Geophysical Observatory, University of Oulu. Characterisation of EMIC/Pc1 waves and monitoring Alfven resonances is also a primary goal of this network. In a recent study ALB, BOU, HRN and ESK stations have been utilized to investigate the evolution of continental-scale lightning activity on the timescale of the El Niño–Southern Oscillation (ENSO) (Williams et al., 2021). In another work long-term changes in the properties of the Earth-ionosphere waveguide have been analyzed based on the HRN, ESK, SHI and VRN stations (Bozóki et al., 2021). The analysed period (13-31 January 2019) was selected based on the availability of data from all the stations listed. The only exception is Mondy (MND) from where data are available only in the 15-30 January period.

Table 1 Detailed information on the 18 SR stations used in the study.

Station	Code	Country	Latitude (°N)	Longitude (°E)	Sampling (Hz)
Alberta	ALB	Canada	51.89	-111.47	130.2
Bharati	BRT	Antarctica	-69.41	76.19	256
Boulder Creek	BOU	USA	37.19	-122.12	130.2
Eskdalemuir	ESK	UK	55.29	-3.17	100
Fort Churchill	FCHU	Canada	58.76	-94.08	100
Hofuf	HOF	Saudi Arabia	25.94	48.95	130.2
Hornsund	HRN	Svalbard	77.0	15.6	100
Hugo	HUG	USA	38.89	-103.40	887.8
Hylaty	HYL	Poland	49.19	22.55	887.8
Kevo	KEV	Finland	69.75	27.02	250
Kilpisjarvi	KIL	Finland	69.05	20.79	250
Ministik Lake	MSTK	Canada	53.35	-112.97	100
Mondy	MND	Russia	51.6	100.9	64
Northland	NOR	New Zealand	-35.11	173.49	130.2
Patagonia	PAT	Argentina	-51.59	-69.32	887.8
Shillong	SHI	India	25.6	91.9	64
Sodankyla	SOD	Finland	67.43	26.39	250
Vernadsky	VRN	Antarctica	-65.25	-64.25	320

In the following we describe how to obtain the quasi-global invariant quantity from SR measurements. All the raw SR time series were processed in the same way. First, standardized one-hour time series have been generated from raw data files with different formats. In this step, the measured data were filtered using a finite impulse response (FIR) bandpass filter, which also corrected for the amplitude response of the recording systems. For the Heartmath stations (ALB, BOU, HOF, NOR), the amplitude-response function is flat in the SR band, so no correction was applied. For the stations of the Finnish pulsation magnetometer chain (KEV, KIL, SOD), the amplitude response of the measuring system is not known. For the WERA stations (HUG, HYL, PAT) a color noise (1/f type noise) appears in the measurements (see Fig.2 in Mlynarczyk et al., 2017) which cannot be corrected by the amplitude response function, so no correction was applied. Based on the bandwidths of the measuring systems and the available information about the amplitude responses, the bandpasses of the FIR filters has been chosen to be 2-45 Hz for the ALB, BOU, ESK, HOF, HRN, HUG, HYL, NOR, PAT and VRN stations, 2-31 Hz for the FCHU, MSTK, KEV, KIL and SOD stations, and 2-30 Hz for the BRT, MND and SHI stations. For the three stations with geomagnetic orientation (FCHU, MSTK, MND) a digital antenna rotation has been applied (Mlynarczyk et al., 2015) when generating the standardized time series in order to transform the records to the geographical main directions.

As the next step in the overall procedure, sanitized power spectral density (PSD) spectra were calculated from the standardized time series based on Welch's method (Welch, 1967). This method estimates the PSD by dividing the data into overlapping segments, determining the PSD of each segment and averaging them. First, spikes larger than 100 pT (in absolute value) were replaced by nans ("not a number"-s) in the time domain to minimize the aliasing effect of regional lightning activity (Tatsis et al., 2021) and exceptionally intense lightning strokes known as Q-bursts (Guha et al., 2017). PSD spectrograms (dynamic spectra) were calculated with a window length (depending on the sampling frequency of the actual stations) corresponding to ~0.1 Hz frequency resolution and a half-window-length overlap. This step unifies the PSD spectra obtained from stations operating at different sampling frequencies. We refer to one column of the spectrogram (dynamic spectrum) which corresponds to the PSD spectrum of one window as a "spectral segment". Those windows that contained nans resulted in spectral segments with only nans (usually around 1-2% of all the spectral segments). Next, narrowband, anthropogenic noises (Salinas et al., 2022), identified manually for each station, have been removed from the spectra. One further sanitation step has been applied based on the spectral power content (SPC) (the sum of PSD values) (Guha et al., 2017) in the lowest part of the spectrum (<6 Hz) and in the SR band (6-30 Hz or 6-40 Hz depending on the bandwidth of the station) where segments with SPC greater than the average plus one standard deviation (either below 6 Hz or in the SR band) has been removed. This is a strict criterion but its application results in very clear SR spectrograms characteristic of "background" lightning activity, without the influence of nearby or remote but very powerful lightning. If the number of removed spectral segments was greater than 40%, then that hour was labeled "bad quality data" and not used (this number of removed spectral segments is usually between 20% and 30%). Finally, average resonance peaks have been fitted for stations with narrower/wider bandwidth, respectively. Finally, we summed the intensities of the first three resonance modes (~8 Hz, ~14 Hz, ~20 Hz) as the main contributor from each magnetic coil to the quasi-global invariant quantity of central interest in this work.

2.2. Independent Lightning Observations

The characteristics of global lightning activity as inferred from the values of the magnetic intensity for the 19-day long period of 13-31 January 2019 are compared with independent lightning observations provided by three global, ground-based lightning monitoring networks: the World Wide Lightning Location Network (WWLLN), the Global Lightning Detection Network (GLD360) and the Earth Networks Total Lightning Network (ENTLN) as well as satellite-based optical lightning observations carried out by the LIS/OTD instruments (climatological) and the Geostationary Lightning Mapper (GLM) onboard the GOES-16 and GOES-17 satellites. The latter provides lightning locations for the American longitudinal sector (i.e., the Western Hemisphere). Two kinds of WWLLN lightning data (RelocB and AE) are available for the study. Algorithms yielding RelocB and AE data are much the same, based on sferic identification in VLF waveforms, determination of times of group arrivals, finding matching pairs, and event localizing. RelocB is the 'official' WWLLN data product. The criteria and parametrizing of the sferic identification, and selection of stations taken into account in pairing has been somewhat altered in a newer code (AE), where - semi heuristic - lightning energies are also involved as additional derivatives. Energy is not provided by the RelocB. The altered AE algorithm resulted in minor differences between the two sets of identified lightning. LIS/OTD observations are taken from the 0.5°x0.5° High Resolution Monthly Climatology (HRMC) dataset (Cecil, 2006). It is to be noted that the ground-based/satellite-based observations provide strokes/flashes, respectively.

2.3. Earth Networks Thunder Hour

Earth Networks recently released Thunder Hours, a new data product that is available and freely accessible for climate research purposes from 2014 to date (DiGangi et al., 2022). Earth Networks Thunder Hour is defined simply as an hour during which thunder can be heard in a particular area (in this case, within a 15 km radius) and is simulated using total lightning data from a combined set of ENTLN- and WWLLN-detected lightning locations called Earth Networks Global Lightning Detection Network (ENGLN). The dataset is available in 0.05°x0.05° spatial resolution and one of its main strengths is that it helps to reduce the influence of detection efficiency on the lightning climatology (DiGangi et al., 2022). In this study we calculate the total daily number of thunder hours for the whole globe and for the three main lightning chimneys and compare them with the SR-based quasi-global invariant quantity.

2.4. Daily Land-Surface Temperature

Berkeley Earth provides an experimental temperature time series with daily resolution (http://berkeleyearth.lbl.gov/auto/Global/Complete_TAVG_daily.txt) which is called the daily land-surface average anomaly and is produced by the Berkeley Earth averaging method described on their website. In this dataset land-surface temperatures are reported as anomalies relative to the January 1951 - December 1980 average. Although the product is said to be preliminary and could be significantly revised in the future, we consider it a roughly correct indicator of day-to-day changes in the global land temperature.

3. Results

Figure 2 shows the worldwide lightning activity measured by satellites (Fig.2a,b) and by ground-based lightning monitoring networks (Fig.2c,d,e,f). While the LIS/OTD observations show climatological lightning activity for January, all other observations cover the period 13-31 January 2019. In the investigated time interval lightning activity is concentrated in the tropical land regions and in the land areas of the Southern Hemisphere, corresponding to the three main lightning "chimney" regions: the Maritime Continent, Africa and South America. This is consistent with the expectation based on solar heating that in Northern Hemispheric winter months global lightning shifts into the Southern Hemisphere (Christian et al., 2003). The LIS/OTD January climatology (Fig.2a) indicates that the African chimney (with largest activity in the Congo basin) is predominant among the three main chimney regions in January. This expectation is not clearly met in the GLD360 (Fig.2c) and ENTLN (Fig.2d) lightning maps and it is definitely not true in case of the WWLLN observations (Fig.2e,f). Further differences can be identified among GLD360, ENTLN and WWLLN lightning maps. Strong lightning activity is detected by GLD360 and by WWLLN in the eastern equatorial part of Brazil which is less dominant in the ENTLN dataset. On the other hand, ENTLN reports strong lightning activity in the eastern part of South Africa which is less dominant in GLD360 and WWLLN observations. The latter difference between GLD360 and ENTLN could be explained by a higher detection for GLD360 in the Congo basin than that of ENTLN (note the different color scales of the maps). The lightning maps also demonstrate that the WWLLN is unique in the sense that it locates intense lightning events globally, far from ground network coverage (e.g., eastward and westward from Central America). The distribution of GLM detected lightning flashes in South America shows the closest similarity with GLD360 observations. These various observations may be summarized with one important conclusion: detection efficiency is a key unknown in the intercomparison of different lightning observations.

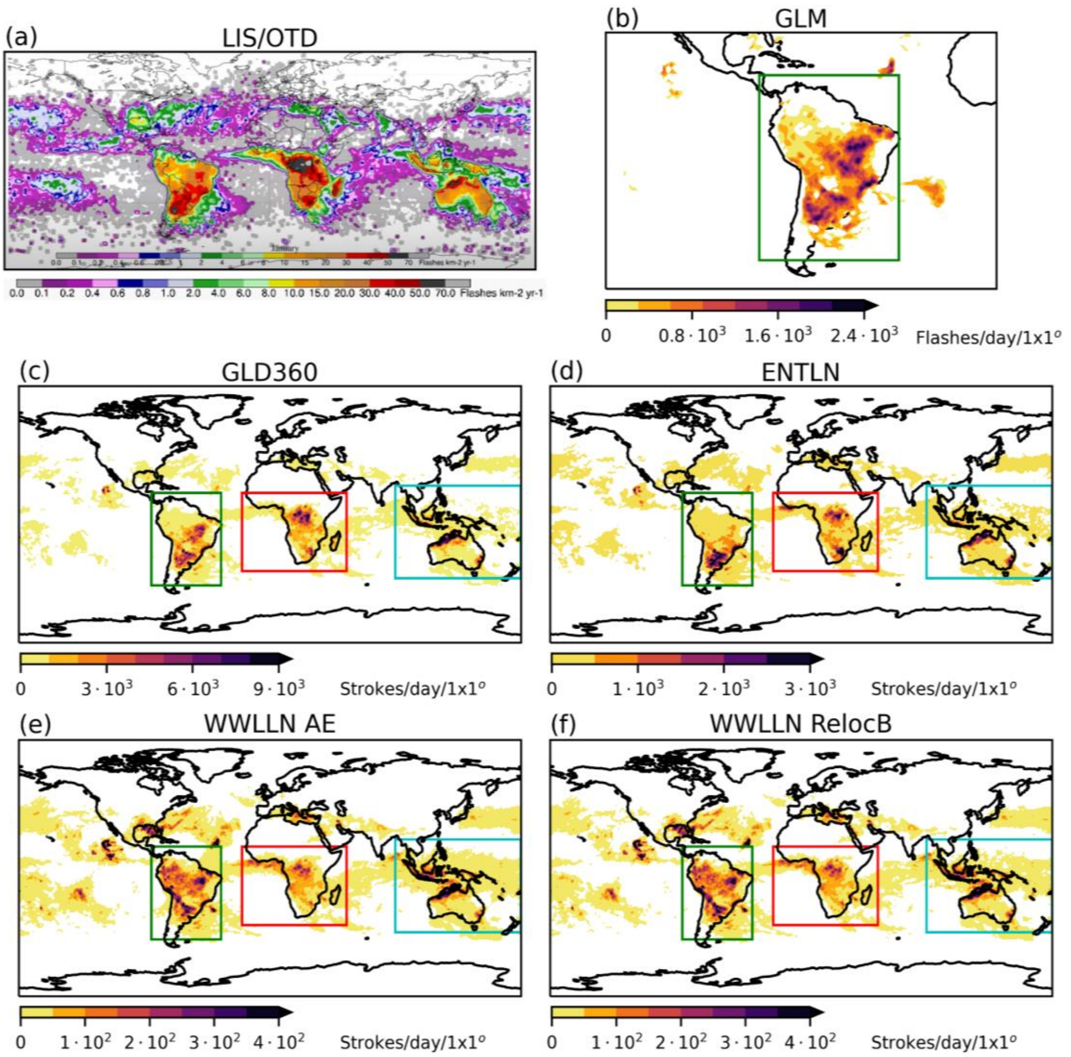

Figure 2. Lightning activity in the 13-31 January 2019 period as seen by different lightning detection methods (except in panel **a** which shows climatological lightning activity for January based on HRMC LIS/OTD observations (Cecil, 2006)). Green (South America), red (Africa) and blue (Maritime Continent) rectangles show those parts of the lightning maps for which stroke/flash numbers and thunder hours are summarized in the chimney-by-chimney analysis (Fig.5 and Fig.6c,d). Note that the upper limits of the color scales are different for the different lightning detection methods.

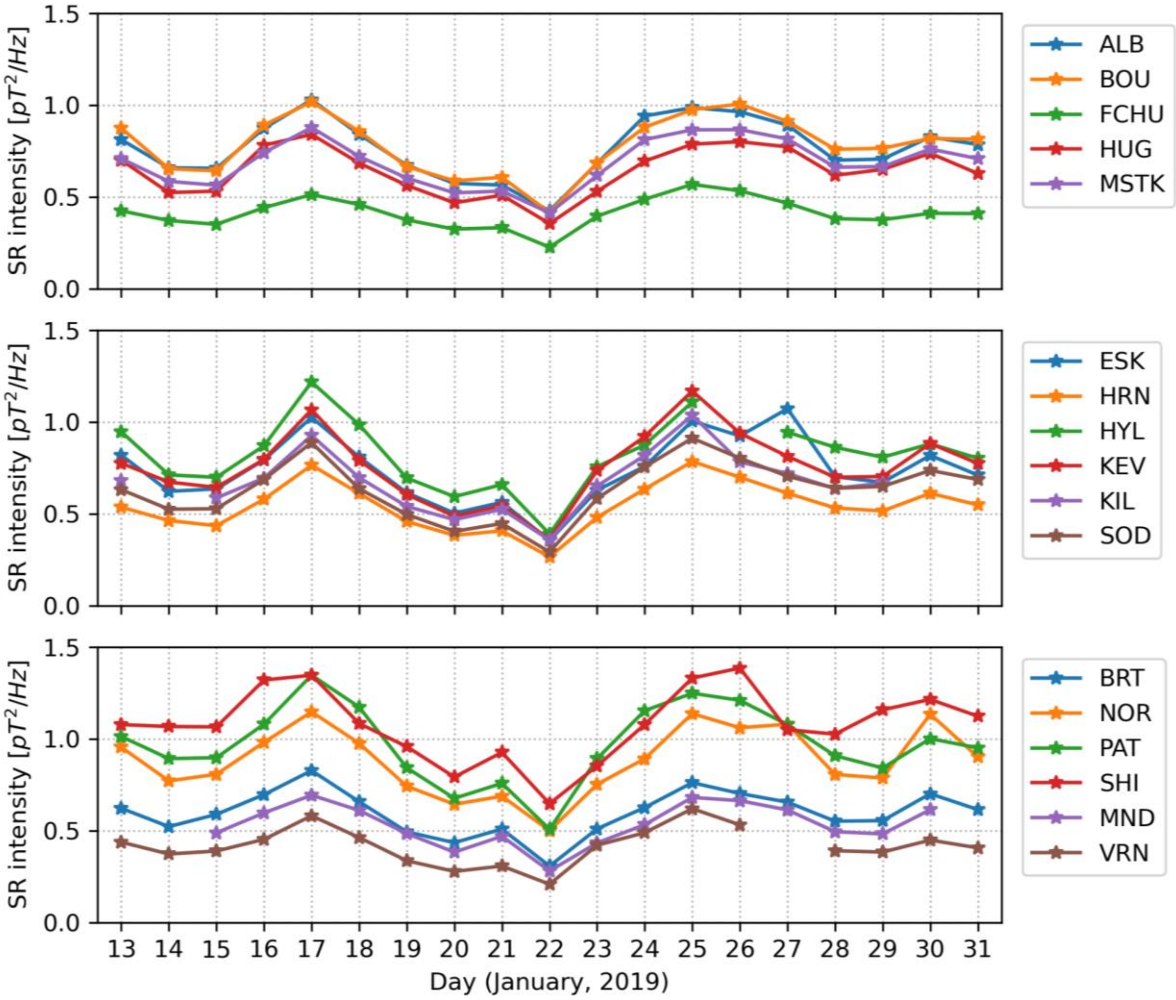

Figure 3. Daily average SR intensity values (the sum of the first three modes and of the two magnetic field components) in the 13-31 January 2019 period. The top panel shows SR intensity records from North America, the middle panel SR intensity records from Europe while the bottom panel SR intensity records from other parts of the globe. A similar behavior of all station records is noted over the 19-day time scale.

Figure 3 shows daily average SR intensity records from 18 stations around the globe. The daily average values are calculated as the sum of the first three SR modes and of the two magnetic field components, in units of pT^2/Hz. The striking similarity between the different records is unambiguous. All of them show a clear maximum on the 17th of January, a well-pronounced minimum on the 22nd of January and a second maximum on the 25-26 of January. A third, smaller maximum can be seen on the 30th of January. SR intensity drops by more than a factor of 2 from 17 to 22 January, i.e. in just 5 days. Given the accumulated evidence that lightning intensity is proportional to SR intensity (e.g., Boldi et al., 2018; Clayton & Polk, 1977), the finding suggests a similar reduction in the overall intensity of global lightning activity over this time interval. The possible origins of this large variation on the day-to-day timescale will be addressed in the Discussion. While the general trends in the different records are very similar, the apparent differences in absolute levels are probably connected to the different distances between the active lightning source regions and the SR stations. Furthermore, some problems probably also arise with the absolute calibration of the magnetic measurements. That is the reason why we call the daily average SR intensity a *quasi-global* invariant quantity. This could possibly be sorted out by similar intercomparisons in different seasons characterized by different source geometries.

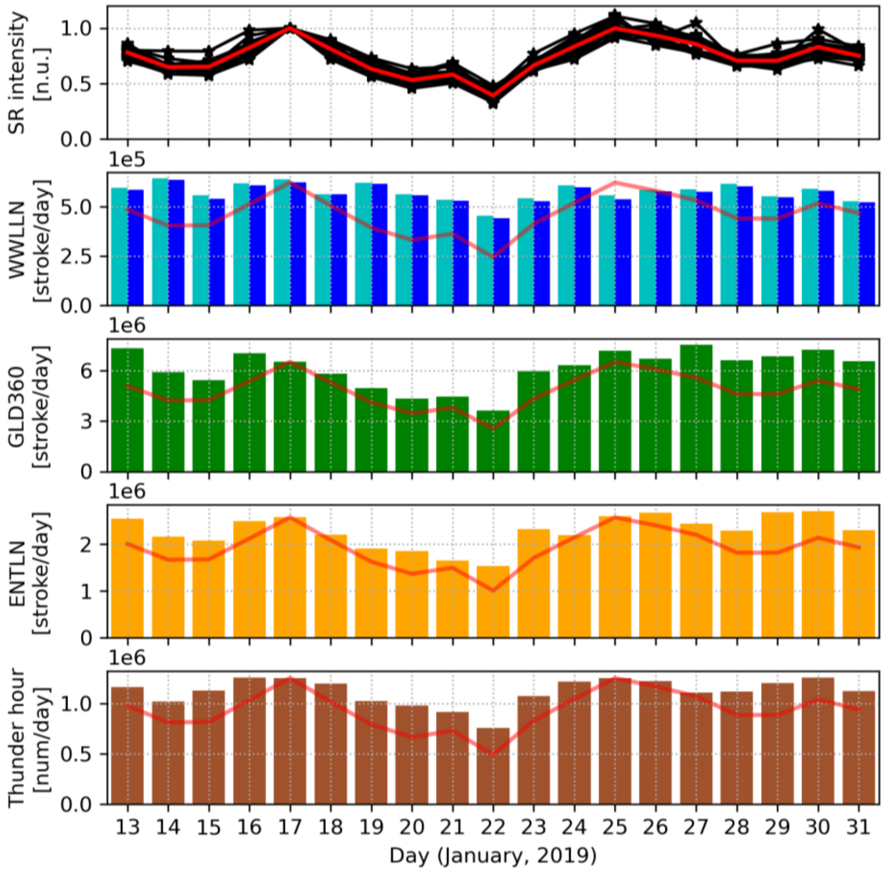

Figure 4. Comparison of normalized daily average SR intensity records (in normalized units) with the total (global) daily stroke rates provided by independent lightning observations (WWLLN, GLD360, ENTLN) and with the total daily numbers of Earth Networks Thunder Hours. In the top subplot black curves correspond to different SR stations while the red curve shows the average of all records. The scaled version of the latter curve is also shown in the other four subplots. In the second row WWLLN RelocB/AE data are shown in cyan/blue, respectively.

Further comparisons with other measures of global lightning activity over the same 19 day interval are shown in Fig.4. In the top row all the daily average SR intensity records from Fig.3 are displayed but now by applying a normalization with respect to the daily average value on the 17th of January. This step reduces the source-observer distance dependence and calibration problems and makes the high degree of similarity among the different SR intensity records even more obvious. The second, third, fourth and fifth subpanels show the total (global) daily stroke rates provided by the WWLLN (cyan/blue: RelocB/AE), GLD360, and ENTLN as well as the total daily numbers of Earth Networks Thunder Hours. Note that the limits of the y axis are different for the different lightning detection networks. GLD360 reports about 3 times more events than ENTLN and more than 10 times more events than WWLLN. GLD360 and ENTLN data follow the general trend of the normalized average SR intensity record quite well (correlation coefficients are: 0.81 and 0.83 for GLD360 and ENTLN, respectively) and are both superior in this aspect in comparison with WWLLN (correlation coefficients are: 0.52 and 0.48 for WWLLN RelocB and AE, respectively). WWLLN RelocB provides about 15% higher daily stroke rates than WWLLN AE but the general trends (day-to-day variations) are very similar in the two datasets. Since the WWLLN is most efficient at detecting high amplitude lightning, this observation may suggest that the day-to-day variation of high amplitude lightning is different from the day-to-day variation of the "average" lightning that maintains SRs. The total daily numbers of Earth Networks Thunder Hours yield the best correlation coefficient with the average SR intensity record: 0.89.

It is to be noted that the relative variation of SR intensity records is considerably larger (more than a factor of 2) than that of other lightning records (usually less than a factor of 2). In Table 2 percentage variations of SR intensity are compared with the different lightning observations for those selected days when SR intensity shows the two largest maxima on 17 and 25 January as well as a pronounced minimum on 22 January. The largest percentage increase/decrease appears in the average SR intensity and in the GLM records (Table 2) while the smallest increase/decrease in the WWLLN observations.

Table 2. Percentage changes in average SR intensity and in other lightning observations between 17 and 22 January as well as between 22 and 25 January.

January days	SR	WWLLN AE	WWLLN RelocB	GLD360	ENTLN	Thunder hour	GLM
17 → 22	-61 %	-29 %	-29 %	-44 %	-40 %	-40%	-52 %
22 → 25	+113 %	+36 %	+34 %	+74 %	+43 %	+61%	+107%

Figure 5 represents the contributions of individual continental chimneys to the global variations in Figs. 3 and 4. It presents SR intensity and independent lightning observations from day to day for the three main lightning chimney regions (the Maritime Continent, Africa and South America) in the time intervals (Maritime Continent: 7-11 UT, Africa: 13-17 UT, South America: 18-22 UT) when lightning activity is the strongest in the respective chimney region (local afternoon hours). The top row shows normalized SR intensity records for selected stations and field components for which the corresponding wave propagation path crosses the actual chimney region (see the Supplementary material for details). On each day SR magnetic intensities are averaged for the first three modes in pT^2/Hz in the time intervals indicated in the top of the figure. The day-to-day changes are different for the three main chimney regions although clear similarities can also be observed between pairs of records. There is again a very high similarity among the SR intensity records from different stations confirming the global representativeness of SR intensity in any time intervals (hours) of a day.

In case of the independent lightning observations (second, third, fourth and fifth rows of Fig.5), lightning strokes and thunder hours are summarized for the same time intervals as SR intensities within the color-coded rectangles marked in Fig.2. We suppose that these areas contain the main lightning sources for SR intensity. Figure 5 reveals that it is the diminishment of African lightning activity on 22 January that causes the minimum in global lightning activity identified in Fig.4. South American lightning activity is also reduced on this day but this reduction starts a few days earlier. The high correlation between GLD360 and ENTLN for the total (global) daily stroke rates (0.93) drops considerably in this chimney-by-chimney analysis (Maritime Continent: 0.78, Africa: 0.79, South America: 0.34). For the Maritime Continent and South America, it is GLD360 that yields the highest correlation with the average SR intensity record (0.49 and 0.67, respectively), while for Africa the ENTLN stroke rates perform the best in this aspect (0.77). This means that thunder hours are not as representative for SRs on the chimney-scale as they were in the global analysis (Fig.4).

We are also interested in the chimney ranking, i.e. the relative strength of the three main lightning chimney regions. Such information on a day-to-day basis may be important for synoptic meteorology and forecasting. This information is lost in the presented SR intensity records when they are normalized with respect to the average value on the 17th of January. Another problem is that SR intensities strongly depend on the source-observer distance, which hinders us from directly utilizing SR intensity records from multiple stations to infer the chimney ranking. We would need to apply an inversion approach to extract this information from the SR records (see e.g., Prácser et al., 2019; Nelson, 1967; Shvets & Hayakawa, 2011) but this step is out of the scope of the present study. Therefore, we turn to independent lightning observations to investigate the question of chimney ranking. WWLLN indicates that the African chimney has the lowest activity of the three, contrary to the findings of prior studies (e.g., Brooks, 1925), but the African chimney also has the fewest WWLLN receivers of the three. Therefore, this inconsistency could be rooted in detection efficiency issues. The GLD360 and ENTLN daily stroke rates do not show characteristic differences between the three main chimney regions (Fig.5, horizontal black lines). The Asian/African/South American chimneys are the most powerful on 10/5/4 days in the GLD360 dataset and on 7/9/3 days in the ENTLN dataset, respectively. On the other hand, thunder hours show the clear dominance of the African lightning chimney in accordance with LIS/OTD lightning climatology (Fig.2a). From all these results it is clear that the available lightning monitoring techniques do not provide a consistent and reliable ranking of lightning activity in the three main chimney regions.

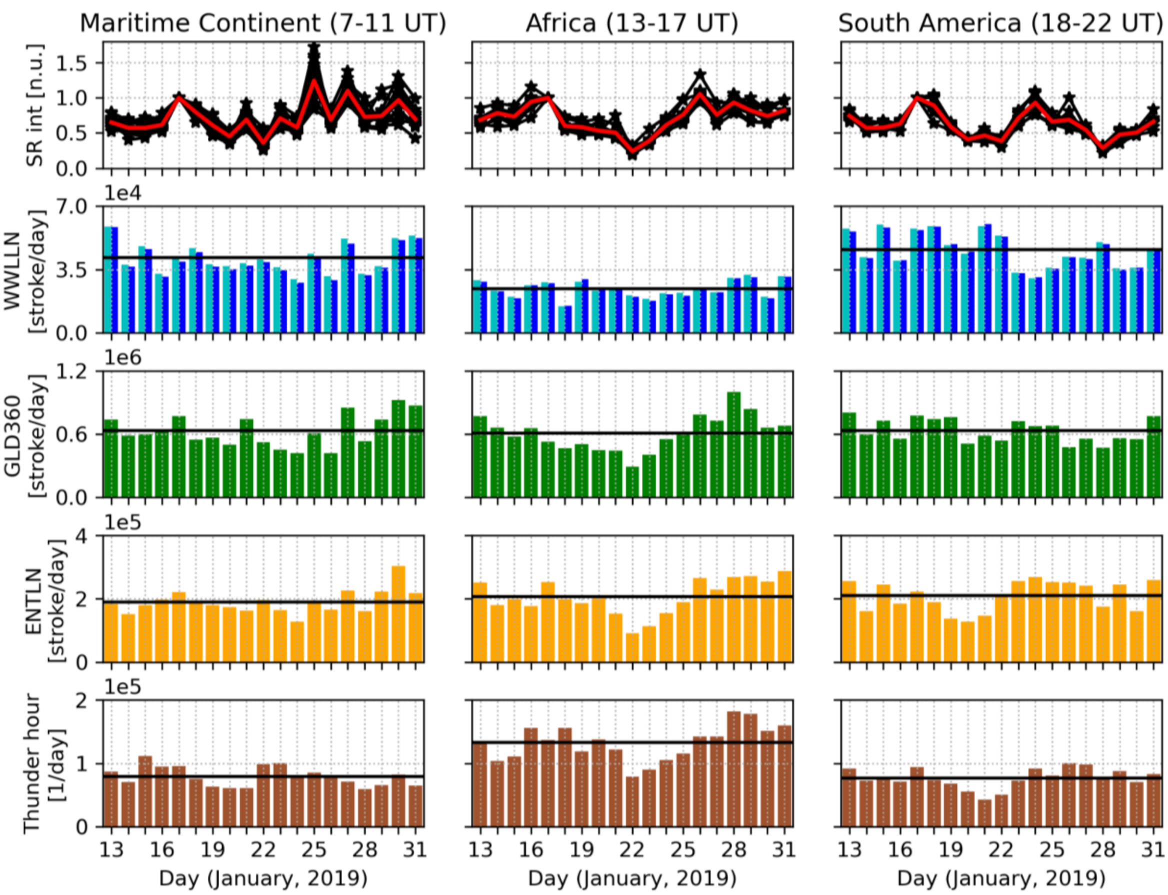

Figure 5. Chimney-by-chimney comparison of normalized average SR intensity records (in normalized units) with stroke rates and thunder hours provided by independent lightning observations (see text for more details). In the top row, black curves correspond to magnetic intensity integrations for different sets of SR stations while the red curve shows the average of all SR stations in each grouping. In the second, third, fourth and fifth rows, horizontal black lines indicate the mean values of the various plotted quantities.

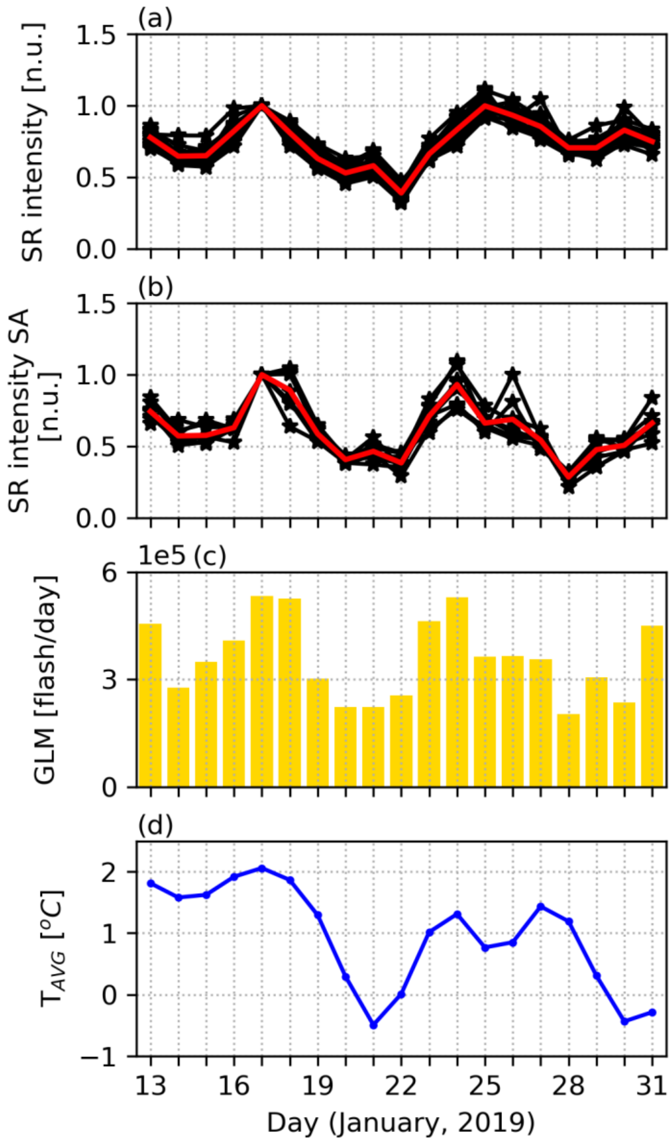

Figure 6. Comparison of (a) normalized daily average SR intensity records (in normalized units) with (b) the normalized average SR intensity records of South America (in normalized units), (c) daily flash rates provided by the GLM instrument and (d) the Berkeley Earth daily land-surface temperature average (TAVG) anomaly. GLM-detected lightning flashes had been summarized within the green rectangle (representing South America) marked in Fig.2.

Figure 6 shows the comparison of normalized daily average SR intensity records for the globe (Fig.6a) with the normalized average SR intensity records of South America (Fig.6b), GLM daily flash rates (Fig.6c) and the Berkeley Earth daily temperature average (TAVG) values (Fig.6d). The daily TAVG anomaly time series clearly shows a similar trend to the daily average SR intensity records i.e., a maximum on 17 January, a minimum on 21 January (this minimum is on 22 January in the SR data) and a second maximum on 24 January (this maximum is on 25 January in the SR data). The inferred overall diminishment in global temperature over four days is ~2.5 C^o, a substantial change. This observation strongly suggests a thermodynamic origin of the global lightning variations indicated by the SR intensity records. Such substantial changes in global temperature are possibly linked to cold air outbreaks

(Hastenrath, 1996) when a large amount of very cold air mass is transported from polar latitudes into warmer regions at low latitudes. There is an excellent agreement between the average SR intensity record corresponding to South America (Fig.6b) and the daily flash rates provided by GLM (Fig.6c). It is noteworthy that the GLM flash counts, representing the entire Western Hemisphere, decline by approximately a factor of two from Jan 17 to Jan 22, in concert with the global quasi-invariant quantity (Fig.6a). The correlation coefficient between these two datasets is 0.93, which is much larger than the correlation between GLM and GLD360/ENTLN (0.69 and 0.63, respectively). This result can be regarded as a validation of our approach for producing quasi-global invariant SR intensity records characterizing individual chimneys.

4. Discussion

Although lightning is recognized now as an essential climate variable by the World Meteorological Organization (WMO) (Aich et al., 2018), the continuous monitoring of global lightning activity on the day-to-day timescale is severely limited as indicated by the apparently inconsistent global lightning distributions presented in Fig.2. Satellite observations do not provide global coverage on this timescale while the detection efficiency of available global ground-based lightning monitoring networks is limited, spatially uneven, and generally unknown (just as the location of the receiving stations is not freely accessible in the case of the GLD360 and ENTLN networks). Moreover, the detection efficiency of these networks is not stable but varies from day to day depending on the actual lightning distribution (see Fig. 2 in Bitzer & Burchfield, 2016). Another important manifestation of this limitation is that even simple questions such as “which of the main lightning chimney regions was the strongest on a given day” currently cannot be answered unambiguously (Fig.5). However, it should also be pointed out that the available technologies are constantly improving: for example ENTLN has undergone a very significant processor upgrade since the investigated period (Zhu et al., 2022), and geostationary lightning monitoring will soon be available for the European longitude sector as well (Holmlund et al., 2021).

Of the three global ground-based lightning detection networks studied here, the WWLLN network is clearly the least representative globally, and this is mainly related to its low detection efficiency in Africa (Fig.5) (Williams & Mareev, 2014). With GLD360 reporting three times as many events as ENTLN (Fig.4) and showing better agreement with GLM data (Fig.2), it is likely that GLD360 was the most reliable and globally representative ground-based lightning detection network during the investigated period. However, based on our results, Earth Networks Thunder Hours (based on the ENTLN lightning dataset) is a very promising quantity for investigating day-to-day variations of global lightning activity (Fig.4).

Schumann resonance measurements offer a cost-effective way to monitor global lightning activity. However, SR intensity values do not provide direct information on the distribution of lightning activity at sub-continental scale. For this purpose we plan to use in the future an inversion algorithm aimed to infer the location and intensity of global lightning based on SR measurements (Dyrda et al., 2014; Nelson, 1967; Prácser et al., 2019; Prácser et al., 2022; Shvets et al., 2010; Shvets et al., 2011; Shvets & Hayakawa, 2011; Williams & Mareev, 2014). The main difficulty in interpreting SR measurements is the complicated source-receiver distance dependence of the resonance field (see e.g., Nickolaenko & Hayakawa, 2002). It is a long-standing goal of SR research to derive a scalar quantity, a SR-based “geoelectric index”, that characterizes the overall intensity of global lightning activity by eliminating this source-receiver distance effect (Holzworth & Volland, 1986; Sentman & Fraser, 1991). Our work followed the long recommended strategy of averaging the intensity of the two field components and as many resonance modes as possible (Sentman & Fraser, 1991; Nieckarz et al., 2009).

Several studies have previously analyzed SR intensity data from multiple stations (e.g., Bozóki et al., 2021; Füllekrug & Fraser-Smith, 1996; Price, 2000; Sentman & Fraser, 1991; Williams & Sátori, 2004; Williams et al., 2021), but to the best of our knowledge, this is the first work that shows for many stations that summing the first three modes of the two magnetic components and averaging these values on a daily basis results in a quasi-global invariant quantity. This quantity shows a very good agreement with total (global) daily stroke rates provided by independent lightning observations and with the total daily numbers of Earth Networks Thunder Hours (Fig.4).

Our group sees great potential in comparing different geophysical parameters with the introduced quasi-global invariant quantity on the day-to-day time scale. The latter can be considered as an indicator of the day-to-day changes in the low-latitude atmospheric updraft, and thus it seems appropriate to investigate whether the upper layers of the atmosphere show considerable variability similar to the very significant day-to-day variability in global lightning activity. The work by Price (2000) can be regarded as such an approach where the author used an SR-based quantity as indicator for day-to-day changes in upper tropospheric water vapor. We also see it as an intriguing question whether there is a parameter (e.g., fluctuations in electron density) specific to the low-latitude ionosphere that correlates with the SR-based quantity we introduced.

At this point, some apparent limitations of the introduced SR-based quantity also need to be discussed. One major limitation is that in its current form, the quasi-global invariant quantity is not really suitable for studying longer time periods. The main reason for this statement is that on longer time scales, the source-observer distance effect associated with the seasonal north-south migration of global lightning activity causes significant changes in SR intensity (Nickolaenko et al., 1998) that are not corrected in the current form of the quasi-global invariant quantity. Further investigations are needed to clarify this likely difficulty, but it is recommended that the quantity introduced should only be used within a one-month period. Changes in the properties of the Earth-ionosphere cavity, i.e. the propagation conditions of ELF waves on the even longer interannual time scale (Bozóki et al., 2021), are another challenge that needs to be addressed in the future. Shorter timescale changes in the properties of the Earth-ionosphere cavity associated with space weather, for example connected with energetic electron precipitation (Bozóki et al., 2021), with geomagnetic storms (Pazos et al., 2019; Salinas et al., 2016), with solar proton events (Roldugin et al., 2003; Schlegel and Füllekrug, 1999), and with the solar rotation (Füllekrug & Fraser-Smith, 1996) can also bias the SR-based characterization of global lightning activity. However, in the present study, where a time interval close to the minimum of solar activity was investigated, there is no clear evidence of a significant space weather effect based on comparisons with independent lightning observations.

Observations in this study of global lightning on daily time scales have raised the interest in cold air outbreaks, a mechanism causing a global change in mean surface air temperature on the same time scale. We showed indications for a northern hemisphere winter event, with influence in both the American and the African chimney. The chimney-by-chimney information on lightning activity presented in Fig.5 suggests that the cold air outbreak initiated in the American longitudinal sector and then shifted eastwards and reached the African longitudes. This scenario is supported by surface skin temperature observations (not shown here) indicating that the cold outbreak first impacted the American chimney and then affected the African chimney as the temperature perturbation moved both equatorward and eastward.

In this study, our interest lies primarily in thermodynamic impacts on global lightning. However, given the recognized influence of aerosol on lightning activity (e.g., Williams, 2020), it should be noted that cold air outbreaks can also deliver cleaner polar air to lower latitude locations (e.g., Liu et al., 2019). The satellite-based method of estimating CCN concentration at cloud base height (Rosenfeld et al., 2016) was used to look for reductions in pollution linked with the equatorward motion of polar air in America and Africa, but no obvious signatures were identified.

5. Conclusions

In this paper we showed that by summing the intensity of the first three Schumann resonance (SR) modes of the two magnetic components and by averaging these values on a daily basis, a quasi-global invariant quantity can be obtained that can be used to investigate day-to-day changes in global lightning activity, supporting the earlier suggestion by Sentman & Fraser (1991). This quantity revealed significant variability in the overall intensity of global lightning activity that can occur within a few days and is likely explained by large-scale changes in land-surface temperatures related to cold air outbreaks. Independent global lightning datasets showed good agreement with the variations of the quasi-global invariant quantity. However, for the three main lightning chimneys on Earth the agreement among different lightning observations (including the SR invariant) is significantly worse, which underlines the need for improving the available observation methods and calculation techniques in this respect. An inversion algorithm that could infer the distribution and intensity of global lightning activity based on SR measurements would be very valuable to fill this important gap in our knowledge.

Acknowledgement

This work was supported by the National Research, Development, and Innovation Office, Hungary-NKFIH, project numbers K138824 and FK135115. The work of T. Bozóki was supported by the ÚNKP-21-3 New National Excellence Program of the Ministry for Innovation and Technology from the source of the National Research, Development and Innovation Fund. The authors thank I.R. Mann, D.K. Milling and the rest of the CARISMA team for data. CARISMA is operated by the University of Alberta, funded by the Canadian Space Agency. The authors wish to thank the World Wide Lightning Location Network (http://wwlln.net), a collaboration among over 50 universities and institutions, for providing the lightning location data used in this study. The contribution of E. Williams and Y. Liu was supported by a grant from the US National Science Foundation (Grant # 6942697). A. Potapov's contribution was supported by the project of the RF Ministry of Education and Science, and the data from obs. Mondy were obtained using the equipment of Center of Common Use “Angara” http://ckp-rf.ru/ckp/3056. Measurements at Vernadsky station were funded by “State Special-Purpose Research Program in Antarctica for 2011-2023” MES of Ukraine.

Data Availability Statement

Thunder hour data provided by Earth Networks, in collaboration with WWLLN, are available at http://thunderhours.earthnetworks.com. LIS/OTD data are available online (https://ghrc.nsstc.nasa.gov/pub/lis/climatology/) from the NASA EOSDIS Global Hydrology Resource Center Distributed Active Archive Center Huntsville, Alabama, U.S.A. GLM data for this study were obtained through https://console.cloud.google.com/storage/browser/gcp-public-data-goes-16. The Berkeley Earth daily land-surface temperature anomaly record is available at http://berkeleyearth.org/data/. Eskdalemuir induction coil data are collected by the British Geological Survey and are available at https://www.bgs.ac.uk/services/ngdc/accessions/index.html#item131926. ENTLN/GLD360 data are available for research purposes from Earth Networks/Vaisala upon request. The WWLLN data are available at a nominal cost from http://wwlln.net. Normalized daily average Schumann resonance (SR) intensity data are available at: https://doi.org/10.5281/zenodo.7555111

References

Adhitya, P., Nosé, M., Bulusu, J., Vichare, G., & Sinha, A.K. (2022). Observation of ionospheric Alfven resonator with double spectral resonance structures at low latitude station, Shillong (dipoleL=1.08). *Earth Planets Space*, **74**, 169. https://doi.org/10.1186/s40623-022-01730-2

Aich, V., Holzworth, R., Goodman, G., Price, C., & Williams, E. (2018). Lightning: A New Essential Climate Variable. *EOS*, **99**. https://eos.org/science-updates/lightning-a-new-essential-climate-variable

Albrecht, R.I., Goodman, S.J., Buechler, D.E., Blakeslee, R.J., & Christian, H.J. (2016). Where are the lightning hotspots on Earth? *Bull. Am. Meteorol. Soc.*, **97**(11), 2,051–2,068. https://doi.org/10.1175/BAMS-D-14-00193.1

Balser, M., & Wagner, C.A. (1960). Observation of Earth-ionosphere cavity resonances. *Nature*, **188**(4751), 638–641. https://doi.org/10.1038/188638a0

Barr, R., Llanwyn Jones, D., & Rodger, C.J. (2000). ELF and VLF radio waves. *J. Atmos. Sol. Terr. Phys.*, **62**(17–18), 1689–1718. https://doi.org/10.1016/S1364-6826(00)00121-8

Beggan, C.D., & Musur, M. (2018). Observation of ionospheric Alfvén resonances at 1–30 Hz and their superposition with the Schumann resonances. *J. Geophys. Res.: Space Phys.*, **123**(5), 4202– 4214. https://doi.org/10.1029/2018JA025264

Beirle, S., Koshak, W., Blakeslee, R., & Wagner, T. (2014). Global patterns of lightning properties derived by OTD and LIS. *Nat. Hazards Earth Syst. Sci.*, **14**(10), 2715–2726. https://doi.org/10.5194/nhess-14-2715-2014

Bitzer, P.M., & Burchfield, J.C. (2016). Bayesian techniques to analyze and merge lightning locating system data. *Geophys. Res. Lett.*, **43**(24), 12,605– 12,613. https://doi.org/10.1002/2016GL071951

Blakeslee, R.J., Lang, T.J., Koshak, W.J., Buechler, D., Gatlin, P., Mach, D.M., et al. (2020). Three Years of the Lightning Imaging Sensor Onboard the International Space Station: Expanded Global Coverage and Enhanced Applications. *J. Geophys. Res. Atmos.*, **125**(16). https://doi.org/10.1029/2020JD032918

Blakeslee, R.J., Mach, D.M., Bateman, M.G., & Bailey, J.C. (2014). Seasonal variations in the lightning diurnal cycle and implications for the global electric circuit. *Atmos. Res.*, **135-136**, 228–243. https://doi.org/10.1016/j.atmosres.2012.09.023

Boldi, R., Williams, E., & Guha, A. (2018). Determination of the global-average charge moment of a lightning flash using Schumann resonances and the LIS/OTD lightning data. *J. Geophys. Res. Atmos.*, **123**(1), 108–123. https://doi.org/10.1002/2017JD027050

Bozóki, T., Sátori, G., Williams, E., Mironova, I., Steinbach, P., Bland E.C., et al. (2021). Solar Cycle-Modulated Deformation of the Earth–Ionosphere Cavity. *Front. Earth Sci.*, **9**. https://doi.org/10.3389/feart.2021.689127

Brooks, C.E.P. (1925). *The distribution of thunderstorms over the globe*. Geophys. Mem. London, 24, 147–64.

Burgesser, R.E. (2017). Assessment of the world wide lightning location network (WWLLN) detection efficiency by comparison to the lightning imaging sensor (LIS). *Q. J. R. Meteorolog. Soc.*, **143**(708), 2809–2817. https://doi.org/10.1002/qj.3129

Cecil, D. J., Buechler, D.E., & Blakeslee, R.J. (2014). Gridded lightning climatology from TRMM-LIS and OTD: Dataset description. *Atmos. Res.*, **135-136**, 404–414. https://doi.org/10.1016/j.atmosres.2012.06.028

Cecil, D.J. (2006). LIS/OTD 0.5 Degree High Resolution Monthly Climatology (HRMC). http://dx.doi.org/10.5067/LIS/LIS-OTD/DATA303

Cecil, D.J., Buechler, D.E., & Blakeslee, R.J. (2015). TRMM LIS Climatology of Thunderstorm Occurrence and Conditional Lightning Flash Rates. *J. Clim.*, **28**(16), 6536–6547. https://doi.org/10.1175/JCLI-D-15-0124.1

Chapman, F.W., Llanwyn Jones, D., Todd, J.D.W., & Challinor, R.A. (1966). Observation on the propagation constant of the Earth-ionosphere waveguide in the frequency band 8 kc/s to 16 kc/s. *Radio Sci.*, **1**(11), 1273–1282. https://doi.org/10.1002/rds19661111273

Christian, H.J., Blakeslee, R.J., Boccippio, D.J., Boeck, W.L., Buechler, D.E., Driscoll, K.T., et al. (2003). Global frequency and distribution of lightning as observed from space by the optical transient detector. *J. Geophys. Res.*, **108**(D1), ACL 4-1–ACL 4-15. https://doi.org/10.1029/2002JD002347

Chronis, T., & Koshak, W.J. (2017). Diurnal Variation of TRMM/LIS Lightning Flash Radiances. *Bull. Am. Meteorol. Soc.*, **98**(7), 1453–1470. https://doi.org/10.1175/BAMS-D-16-0041.1

Clayton, M., & Polk, C. (1977). Diurnal Variation and Absolute Intensity of Worldwide Lightning Activity, September 1970 to May 1971. In H. Dolezalek & R. Reiter (Eds.), *Electrical Processes in Atmospheres* (pp. 440). Darmstadt, West Germany: Verlag.

Crossett, C.C., & Metz, N.D. (2017). A Climatological Study of Extreme Cold Surges along the African Highlands. *J. App. Met. Clim.*, **56**, 1731–1738. https://doi.org/10.1175/JAMC-D-15-0191.1

DiGangi, E.A., Stock, M., & Lapierre, J. (2022). Thunder Hours: How Old Methods Offer New Insights into Thunderstorm Climatology. *Bull. Am. Meteorol. Soc.*, **103**(2), E548–E569. https://doi.org/10.1175/BAMS-D-20-0198.1

Dyrda, M., Kulak, A., Mlynarczyk, J., Ostrowski, M., Kubisz, J., Michalec, A., & Nieckarz, Z. (2014). Application of the Schumann resonance spectral decomposition in characterizing the main African thunderstorm center. *J. Geophys. Res. Atmos.*, **119**(23), 13,338–13,349. https://doi.org/10.1002/2014JD022613

Füllekrug, M., & Fraser-Smith, A.C. (1996). Further evidence for a global correlation of the Earth-ionosphere cavity resonances. *Geophys. Res. Lett.*, **23**(20), 2773-2776. https://doi.org/10.1029/96GL02612

Füllekrug, M. (2021a). Global lightning quanta. *J. Geophys. Res. Atmos.*, **126**(9). https://doi.org/10.1029/2020JD033201

Füllekrug, M. (2021b). Simulation of Earth-ionosphere cavity resonances with lightning flashes reported by OTD/LIS. *J. Geophys. Res. Atmos.*, 126(24). https://doi.org/10.1029/2021JD035721

Galejs, J. (1972). *Terrestrial Propagation of Long Electromagnetic Waves*. New York: Pergamon.

Goodman, S.J., Blakeslee, R.J., Koshak, W.J., Mach, D., Bailey, J., Buechler, D., et al. (2013). The GOES-R geostationary lightning mapper (GLM). *Atmos. Res.*, **125-126**, 34–49. https://doi.org/10.1016/j.atmosres.2013.01.006

Guha, A., Williams, E., Boldi, R., Sátori, G., Nagy, T., Bór, J., et al. (2017). Aliasing of the Schumann Resonance Background Signal by Sprite-Associated Q-Bursts. *J. Atmos. Solar-Terrestrial Phys.*, **165-166**, 25–37. https://doi.org/10.1016/j.jastp.2017.11.003

Haldoupis, C., Rycroft, M., Williams, E., & Price, C. (2017). Is the “Earth-ionosphere capacitor” a valid component in the atmospheric global electric circuit? *J. Atmos. Sol. Terr. Phys.*, **164**, 127–131. https://doi.org/10.1016/j.jastp.2017.08.012

Hansen, J., & Lebedeff, S. (1987). Global trends of measured surface air temperature. *J. Geophys. Res.*, **92**(D11), 13,345–13,372. https://doi.org/10.1029/JD092iD11p13345

Hartjenstein, G.& Block, G.B. (1991). Factors affecting cold-air outbreaks east of the Rocky Mountains. *Mon. Wea. Rev.*, **119**, 2280–2292. https://doi.org/10.1175/1520-0493(1991)119<2280:FACAOE>2.0.CO;2

Hastenrath, S., ‘Cold surges’, Section 7.9 in *Climate Dynamics of the Tropics*, Kluwer Academic Publishers, Reprinted 1996.

Heckman, S., Williams, E., & Boldi, R. (1998). Total global lightning inferred from Schumann resonance measurements. *J. Geophys. Res.*, **103**(D24), 31,775–31,779. https://doi.org/10.1029/98JD02648

Holmlund, K., Grandell, J., Schmetz, J., Stuhlmann, R., Bojkov, B., Munro, R., et al. (2021). Meteosat Third Generation (MTG): Continuation and Innovation of Observations from Geostationary Orbit. *Bull. Am. Meteorol. Soc.*,**102**(5), E990–E1015. https://doi.org/10.1175/BAMS-D-19-0304.1

Holzworth, R.H., Brundell, J.B., McCarthy, M.P., Jacobson, A.R., Rodger, C.J., & Anderson, T.S. (2021). Lightning in the Arctic. *Geophys. Res. Lett.*, **48**(7). https://doi.org/10.1029/2020GL091366

Holzworth, R.H., McCarthy, M.P., Brundell, J.B., Jacobson, A.R., & Rodger, C.J. (2019). Global distribution of superbolts. *J. Geophys. Res. Atmos.*, **124**(17-18), 9,996–10,005. https://doi.org/10.1029/2019JD030975

Holzworth, R., & Volland, H. (1986). Do we need a geoelectric index? *Eos Trans. AGU*, **67**(26), 545–548. https://doi.org/10.1029/EO067i026p00545-01

Hutchins, M.L., Holzworth, R.H., Brundell, J.B., & Rodger, C.J. (2012). Relative detection efficiency of the World Wide Lightning Location Network. *Radio Sci.*, **47**(6). https://doi.org/10.1029/2012RS005049

Hutchins, M.L., Jacobson, A.R., Holzworth, R.H., & Brundell, J. B. (2013). Azimuthal dependence of VLF propagation. *J. Geophys. Res.: Space Phys.*, **118**(9), 5808–5812. https://doi.org/10.1002/jgra.50533

Jackson, J.D. (1975). *Classical Electrodynamics*, second ed. Wiley, New York, NY. https://cds.cern.ch/record/100964

Kakad, B., Omura, Y., Kakad, A., Upadhyay, A., & Sinha, A.K. (2018). Characteristics of subpacket structures in ground EMIC wave observations. *J. Geophys. Res.: Space Phys.*, **123**(10), 8358–8376. https://doi.org/10.1029/2018JA025473

Kim, H., Hwang, J., Park, J., Miyashita, Y., Shiokawa, K., Mann, I.R., Raita, T., & Lee, J. (2018). Large-scale ducting of Pc1 pulsations observed by Swarm satellites and multiple ground networks. *Geophys. Res. Lett.*, **45**(23), 12,703–12,712. https://doi.org/10.1029/2018GL080693

Koloskov, A.V., Nickolaenko, A.P., Yampolsky, Y.M., Yu, C., Budanov, O.V., & Budanov, O.V. (2020). Variations of Global Thunderstorm Activity Derived from the Long-Term Schumann Resonance Monitoring in the Antarctic and in the Arctic. *J. Atmos. Sol. Terr. Phys.*, **201**, 105231. https://doi.org/10.1016/j.jastp.2020.105231

Koloskov, O.V., Nickolaenko, A.P., Yampolski, Y.M., & Budanov, O.V. (2022). Electromagnetic seasons in Schumann resonance records. *J. Geophys. Res. Atmos.*, **127**(17), e2022JD036582. https://doi.org/10.1029/2022JD036582

Kousky, V.E. (1979). Frontal influences on Northeast Brazil. *Mon. Wea. Rev.*, **107**, 1140–1153. http://dx.doi.org/10.1175/1520-0493(1979)107<1140:FIONB>2.0.CO;2

Kulak, A., Kubisz, J., Klucjasz, S., Michalec, A., Mlynarczyk, J., Nieckarz, Z., et al. (2014). Extremely low frequency electromagnetic field measurements at the Hylaty station and methodology of signal analysis. *Radio Sci.*, **49**(6), 361–370. https://doi.org/10.1002/2014RS005400

Kulak, A., Mlynarczyk, J., Zieba, S., Micek, S., & Nieckarz, Z. (2006). Studies of ELF propagation in the spherical shell cavity using a field decomposition method based on asymmetry of Schumann resonance curves. *J. Geophys. Res.: Space Phys.*, **111**(A10). https://doi.org/10.1029/2005JA011429

Lanfredi, I.S., & de Camargo, R. (2018). Classification of extreme cold incursions over South America. *Weather and Forecasting*, **33**, 1183–1203. https://doi.org/10.1175/WAF-D-17-0159.1

Liu, Q., Chen, G., & Iwasaki, T. (2019). Quantifying the impacts of cold airmass on aerosol concentrations over North China using isentropic analysis. *J. Geophys. Res. Atmos.*, 124(13), 7308–7326. https://doi.org/10.1029/2018JD029367

Lupo, A.R., Nocera, J.J., Bosart, L.F., Hoffman, E.G., & Knight, D.J. (2001). South American Cold Surges: Types, Composites, and Case Studies. *Mon. Weather Rev.*, **129**(5), 1021–1041. https://doi.org/10.1175/1520-0493(2001)129<1021:SACSTC>2.0.CO;2

Lyons, W.A., Bruning, E.C., Warner, T.A., MacGorman, D.R., Edgington, S., Tillier, C., & Mlynarczyk, J. (2020). Megaflashes: Just How Long Can a Lightning Discharge Get? *Bull. Am. Meteorol. Soc.*, **101**(1), E73–E86. https://doi.org/10.1175/BAMS-D-19-0033.1

Madden, T., & Thompson, W. (1965). Low-frequency electromagnetic oscillation of the Earth-ionosphere cavity. *Rev. Geophys.*, **3**(2), 211–254. https://doi.org/10.1029/RG003i002p00211

Mann, I. R., Milling, D.K., Rae, I.J., Ozeke, L.G., Kale, A., Kale, Z.C., et al. (2008). The upgraded CARISMA magnetometer array in the THEMIS era. *Space Sci. Rev.*, **141**, 413–451. https://doi.org/10.1007/s11214-008-9457-6

Marchand, M., Hilburn, K., & Miller, S. D. (2019). Geostationary lightning mapper and Earth networks lightning detection over the contiguous United States and dependence on flash characteristics. *J. Geophys. Res. Atmos.*, **124**(21), 11552–11567. https://doi.org/10.1029/2019JD031039

Marchenko, V., Mlynarczyk, J., Ostrowski, M., Kulak, A., Senchenko, O., Kubisz, J., et al. (2021). Study of a TGF associated with an Elve using extremely low frequency electromagnetic waves. *J. Geophys. Res. Atmos.*, **126**(3), e2020JD033070. https://doi.org/10.1029/2020JD033070

Marchuk R.A., Potapov A.S., Mishin V. . (2022). Synchronous globally observable ultrashort-period pulses. *Solar-Terrestrial Physics*, **8**(2), 47–55. https://doi.org/10.12737/stp-82202207

Marengo, J., Cornejo, A., Satyamurty, P., Nobre, C., & Sea, W. (1997). Cold Surges in Tropical and Extratropical South America: The Strong Event in June 1994. *Mon. Weather Rev.*, **125**(11), 2759–2786. https://doi.org/10.1175/1520-0493(1997)125<2759:CSITAE>2.0.CO;2

Markson, R. (2007). The Global Circuit Intensity: Its Measurement and Variation over the Last 50 Years. *Bull. Am. Meteorol. Soc.*, **88**(2), 223–242. https://doi.org/10.1175/BAMS-88-2-223

Matsuda, S., Miyoshi, Y., Kasahara, Y., Blum, L., Colpitts, C., Asamura, K., et al. (2021). Multipoint measurement of fine-structured EMIC waves by Arase, Van Allen Probe A, and ground stations. *Geophys. Res. Lett.*, **48**(23), e2021GL096488. https://doi.org/10.1029/2021GL096488

Metz, N.D., Archambault, H.M., Shrock, A.F., Galarneau, T. J. Jr., Bosart, L.F. (2013). A Comparison of South American and African Preferential Pathways for Extreme Cold. *Mon. Weather Rev.*, **141**, 2066–2086. https://doi.org/10.1175/MWR-D-12-00202.1

Mlynarczyk, J., Bór, J., Kulak, A., Popek, M., & Kubisz, J. (2015). An unusual sequence of sprites followed by a secondary TLE: An analysis of ELF radio measurements and optical observations. *J. Geophys. Res.: Space Phys.*, **120**(3), 2241–2254. https://doi.org/10.1002/2014JA020780

Mlynarczyk, J., Kulak, A., & Salvador, J. (2017). The accuracy of radio direction finding in the extremely low frequency range. *Radio Sci.*, **52**(10), 1245– 1252. https://doi.org/10.1002/2017RS006370

Murakami, T. (1979). Winter monsoonal surges over East and Southeast Asia. *J. Met. Soc., Japan*, **57**, 133–158.

Musur, M. A., & Beggan, C. D. (2019). Seasonal and Solar Cycle Variation of Schumann Resonance Intensity and Frequency at Eskdalemuir Observatory, UK. Sun and Geosphere, 14(1). https://doi.org/10.31401/SunGeo.2019.01.11

Nelson, P.H. (1967). *Ionospheric perturbations and Schumann resonance data*. Project NR-371-401. (PhD dissertation), Cambridge, MA:Geophysics Laboratory, Massachusetts Institute of Technology.

Neska, M., Czubak, P., & Reda, J. (2019). Schumann Resonance Monitoring in Hornsund (Spitsbergen) and Suwałki (Poland). Publs. Inst. Geophys. P.A.S. 425, 41–45. https://doi.org/10.25171/InstGeoph_PAS_Publs-2019-008

Nickolaenko, A.P., & Hayakawa, M. (2002). *Resonances in the Earth-Ionosphere Cavity*. Dordrecht: Kluwer.

Nickolaenko, A.P., & Rabinowicz, L.M. (1995). Study of the annual changes of global lightning distribution and frequency variations of the first Schumann resonance mode. *J. Atmos. Terr. Phys.*, **57**(11), 1345–1348. https://doi.org/10.1016/0021-9169(94)00114-4

Nickolaenko, A.P., Sátori, G., Zieger, B., Rabinowicz, L.M., Kudintseva, I.G. (1998). Parameters of global thunderstorm activity deduced from long-term Schumann resonance records. *J. Atmos. Sol. Terr. Phys.*, **60**(3), 387–399. https://doi.org/10.1016/S1364-6826(97)00121-1

Nieckarz, Z., Kułak, A., Zięba, S., Kubicki, M., Michnowski, S., & Barańskiaverage, P. (2009). Comparison of global storm activity rate calculated from Schumann resonance background components to electric field intensity E0Z. *Atmos. Res.*, **91**(2-4), 184–187. https://doi.org/10.1016/j.atmosres.2008.06.006

Pazos, M., Mendoza, B., Sierra, P., Andrade, E., Rodríguez, D., Mendoza, V., et al. (2019). Analysis of the Effects of Geomagnetic Storms in the Schumann Resonance Station Data in Mexico. *J. Atmos. Solar-Terrestrial Phys.*, **193**, 105091. https://doi.org/10.1016/j.jastp.2019.105091

Peterson, M., Mach, D., & Buechler, D. (2021). A global LIS/OTD climatology of lightning Flash Extent Density. *J. Geophys. Res. Atmos.*, **126**(8). https://doi.org/10.1029/2020JD033885

Plotnik, T., Price, C., Saha, J., & Guha, A. (2021). Transport of Water Vapor from Tropical Cyclones to the Upper Troposphere. *Atmosphere*. **12**(11), 1506. https://doi.org/10.3390/atmos12111506

Prácser, E., & Bozóki, T. (2022). On the reliability of the inversion aimed to reconstruct global lightning activity based on Schumann resonance measurements. *J. Atmos. Sol. Terr. Phys.*, **235**, 105892. https://doi.org/10.1016/j.jastp.2022.105892

Prácser, E., Bozóki, T., Sátori, G., Williams, E., Guha, A., & Yu, H. (2019). Reconstruction of Global Lightning Activity Based on Schumann Resonance Measurements: Model Description and Synthetic Tests. *Radio Sci.*, **54**(3), 254–267. https://doi.org/10.1029/2018RS006772

Price, C. (2000). Evidence for a link between global lightning activity and upper tropospheric water vapour. *Nature*, **406**, 290–293. https://doi.org/10.1038/35018543

Price, C. (2016). ELF electromagnetic waves from lightning: The Schumann resonances. *Atmosphere*, **7**(9). https://doi.org/10.3390/atmos7090116

Price, C., Penner, J., & Prather, M. (1997). NOx from lightning: 1. Global distribution based on lightning physics. *J. Geophys. Res.*, **102**(D5), 5929–5941. https://doi.org/10.1029/96JD03504

Prince, K.C., & Evans, C. (2018). A Climatology of Extreme South American Andean Cold Surges. *J. App. Met. Clim.*, **57**, 2297–2315. https://doi.org/10.1175/JAMC-D-18-0146.1

Roldugin, V.C., Maltsev, Y.P., Vasiljev, A.N., Shvets, A.V., & Nikolaenko, A.P. (2003). Changes of Schumann Resonance Parameters During the Solar Proton Event of 14 July 2000. *J. Geophys. Res.: Space Phys.*, **108**(A3). https://doi.org/10.1029/2002JA009495

Rosenfeld, D., Zheng, Y., Hashimshoni, E., Pöhlker, M.L., Jefferson, A., Pöhlker, C. et al. (2016). Satellite retrieval of cloud condensation nuclei concentrations by using clouds as CCN chambers. *PNAS*, **113**(21). https://doi.org/10.1073/pnas.1514044113

Rudlosky, S. D. (2015). Evaluating ENTLN performance relative to TRMM/LIS. *J. Operational Meteor.*, **3**(2), 1120. http://dx.doi.org/10.15191/nwajom.2015.0302

Salinas, A., Toledo-Redondo, S., Navarro, E.A., Fornieles-Callejón, J., and Portí, J.A. (2016). Solar Storm Effects During Saint Patrick's Days in 2013 and 2015 on the Schumann Resonances Measured by the ELF Station at Sierra Nevada (Spain). *J. Geophys. Res. Space Phys.*, **121**(12), 12,234-12,246. https://doi.org/10.1002/2016JA023253

Salinas, A., Rodríguez-Camacho, J., Portí, J., Carrión, M.C., Fornieles-Callejón, J., Toledo-Redondo, S. (2022). Schumann resonance data processing programs and four-year measurements from Sierra Nevada ELF station. Comput. Geosci., **165**, 105148. https://doi.org/10.1016/j.cageo.2022.105148

Sátori, G. (1996). Monitoring Schumann resonances-II. Daily and seasonal frequency variations. *J. Atmos. Terr. Phys.*, **58**(13), 1,483–1,488. http://dx.doi.org/10.1016/0021-9169(95)00146-8

Sátori, G., & Zieger, B. (1999). El Niňo related meridional oscillation of global lightning activity. *Geophys. Res. Lett.*, **26**(10), 1365–1368. https://doi.org/10.1029/1999GL900264

Sátori, G., & Zieger, B. (2003). Areal Variations of the Worldwide Thunderstorm Activity on Different Time Scales as Shown by Schumann Resonances. In: Serge Chauzy, Pierre Laroche (ed.) *Proceeding of the 12th ICAE*, Global Lightning and Climate. Versailles, France, 2003.06.09-2003.06.13. pp. 765-768.

Sátori, G., Williams, E., & Lemperger, I. (2009). Variability of global lightning activity on the ENSO time scale. *Atmos. Res.*, **91**(2-4), 500–507. http://dx.doi.org/10.1016/j.atmosres.2008.06.014

Sátori, G., Neska, M., Williams, E., & Szendrői, J. (2007). Signatures of the day-night asymmetry of the Earth-ionosphere cavity in high time resolution Schumann resonance records. *Radio Sci.*, **42**(2), RS2S10. https://doi.org/10.1029/2006RS003483

Sátori, G., Williams, E., Price, C., Boldi, R., Koloskov, A., Yampolski, Y., et al. (2016). Effects of Energetic Solar Emissions on the Earth-Ionosphere Cavity of Schumann Resonances. *Surv. Geophys.*, **37**, 757–789. https://doi.org/10.1007/s10712-016-9369-z

Schlegel, K., & Füllekrug, M. (1999). Schumann Resonance Parameter Changes during High-Energy Particle Precipitation. *J. Geophys. Res. Space Phys.*, **104**(A5), 10,111–10,118. https://doi.org/10.1029/1999JA900056

Schumann, U., & Huntrieser, H. (2007). The global lightning-induced nitrogen oxides source. *Atmos. Chem. Phys.*, **7**, 3823–3907. https://doi.org/10.5194/acp-7-3823-2007

Schumann, W.O. (1952). Über die strahlungslosen Eigenschwingungen einer leitenden Kugel, die von einer Luftschicht und einer Ionosphärenhülle umgeben ist. *Zeitschrift für Naturforschung*, **7**(2), 149–154. https://doi.org/10.1515/zna-1952-0202

Sentman, D.D., & Fraser, B.J. (1991). Simultaneous observations of Schumann resonances in California and Australia: Evidence for intensity modulation by the local height of the D region. *J. Geophys. Res.*, **96**(A9), 15973–15984. https://doi.org/10.1029/91JA01085

Shvets, A.V., & Hayakawa, M. (2011). Global lightning activity on the basis of inversions of natural ELF electromagnetic data observed at multiple stations around the world. *Surv. Geophys.*, **32**(6), 705–732. https://doi.org/10.1007/s10712-011-9135-1

Shvets, A. V., Hayakawa, M., Sekiguchi, M., & Ando, Y. (2009). Reconstruction of the global lightning distribution from ELF electromagnetic background signals. *J. Atmos. Sol. Terr. Phys.*, **71**(12), 1405–1412. https://doi.org/10.1016/j.jastp.2009.06.008

Shvets, A. V., Hobara, Y., & Hayakawa, M. (2010). Variations of the global lightning distribution revealed from three-station Schumann resonance measurements. *J. Geophys. Res.: Space Phys.*, **115**, A12316. https://doi.org/10.1029/2010JA015851

Strumik, M., Slominski, J., Slominska, E., Mlynarczyk, J., Blecki, J., Haagmans, R., et al. (2021). Experimental evidence of a link between lightning and magnetic field fluctuations in the upper ionosphere observed by Swarm. *Geophys. Res. Lett.*, **48**(4), e2020GL091507. https://doi.org/10.1029/2020GL091507

Tatsis, G., Sakkas, A., Christofilakis, V., Baldoumas, G., Chronopoulos, S.K., Paschalidou, A.K., et al. (2021). Correlation of Local Lightning Activity with Extra Low Frequency Detector for Schumann Resonance Measurements. *Sci. Total Environ.*, **787**, 147671. https://doi.org/10.1016/j.scitotenv.2021.147671

Taylor, W.L. (1960). VLF attenuation for east-west and west-east daytime propagation using atmospherics. *J. Geophys. Res.*, **65**(7), 1933–1938. https://doi.org/10.1029/JZ065i007p01933

Timofejeva, I., McCraty, R., Atkinson, M., Alabdulgader, A.A., Vainoras, A., Landauskas, M., Šiaučiūnaitė, V., Ragulskis, M. (2021). Global Study of Human Heart Rhythm Synchronization with the Earth's Time Varying Magnetic Field. *Appl. Sci.*, **11**, 2935. https://doi.org/10.3390/app11072935

Virts, K.S., Wallace, J.M., Hutchins, M.L., & Holzworth, R.H. (2013). Highlights of a New Ground-Based, Hourly Global Lightning Climatology. *Bull. Am. Meteorol. Soc.*, **94**(9), 1381–1391. https://doi.org/10.1175/BAMS-D-12-00082.1

Wait, J.R. (1970). *Electromagnetic Wave in Stratified Media*. The Institute of Electrical and Electronics Engineers Inc. New York: Oxford University Press Oxford.

Welch, P. (1967). The Use of Fast Fourier Transform for the Estimation of Power Spectra: A Method Based on Time Averaging over Short, Modified Periodograms. *IEEE Trans. Audio Electroacoust.*, **15**(2), 70–73. https://doi.org/10.1109/TAU.1967.1161901

Williams E.R., & Sátori G. (2004). Lightning, thermodynamic and hydrological comparison of two tropical continental chimneys. *J. Atmos. Sol. Terr. Phys.*, **66**, 1213–1231. https://doi.org/10.1016/j.jastp.2004.05.015

Williams, E., Bozóki, T., Sátori, G., Price, C., Steinbach, P., Guha, A., et al. (2021). Evolution of global lightning in the transition from cold to warm phase preceding two super El Niño events. *J. Geophys. Res. Atmos.*, **126**(3). https://doi.org/10.1029/2020JD033526

Williams, E., Guha, A., Boldi, R., Christian, H., & Buechler, D. (2019). Global lightning activity and the hiatus in global warming. *J. Atmos. Sol. Terr. Phys.*, **189**, 27–34. https://doi.org/10.1016/j.jastp.2019.03.011

Williams, E.R. (1992). The Schumann resonance: A global tropical thermometer. *Science*, **256**(5060), 1184–1187. https://doi.org/10.1126/science.256.5060.1184

Williams, E.R. (2005). Lightning and climate: A review. *Atmos. Res.*, **76**(1–4), 272–287. https://doi.org/10.1016/j.atmosres.2004.11.014

Williams, E.R. (2020). Chapter 2: "Lightning and Climate Change" Chapter 2 in book. In A. Piantini (Ed.), *Lightning Interaction with Power Systems*. Stevenage: UK: The Institution of Engineering and Technology.

Williams, E.R., & Mareev, E.A. (2014). Recent progress on the global electrical circuit. *Atmos. Res.*, **135–136**, 208–227. https://doi.org/10.1016/j.atmosres.2013.05.015

Upadhyay, A., Kakad, B., Kakad, A., & Rawat, R. (2022). A statistical study of modulation of electromagnetic ion cyclotron waves observed on ground. *J. Geophys. Res.: Space Phys.*, **127**(8), e2022JA030340. https://doi.org/10.1029/2022JA030340

Yang, J., Zhang, Z., Wei, C., Lu, F., & Guo, Q. (2017). Introducing the New Generation of Chinese Geostationary Weather Satellites, Fengyun-4. *Bull. Am. Meteorol. Soc*., **98**(8), 1637–1658. https://doi.org/10.1175/BAMS-D-16-0065

Zhu, Y., Stock, M., Lapierre, J., & DiGangi, E. (2022). Upgrades of the Earth Networks Total Lightning Network in 2021. *Remote Sens.*, **14**(9), 2209. https://doi.org/10.3390/rs14092209

A Schumann Resonance-based Quantity for Characterizing Day-to-day Changes in Global Lightning Activity

T. Bozóki[1,2], G. Sátori[1], E. Williams[3], A. Guha[4], Y. Liu[3], P. Steinbach[5,6], A. Leal[7,8], M. Atkinson[9], C. D. Beggan[10], E. DiGangi[11], A. Koloskov[12,13], A. Kulak[14], J. LaPierre[11], D.K. Milling[15], J. Mlynarczyk[14], A. Neska[16], A. Potapov[17], T. Raita[18], R. Rawat[19], R. Said[20], A.K. Sinha[21], Y. Yampolski[22]

[1]Institute of Earth Physics and Space Science (EPSS), Sopron, Hungary.

[2]Department of Optics and Quantum Electronics, University of Szeged, Szeged, Hungary.

[3]Parsons Laboratory, Massachusetts Institute of Technology, Cambridge, Massachusetts, USA.

[4]Department of Physics, Tripura University, Agartala, India.

[5]Department of Geophysics and Space Science, Eötvös Loránd University, Budapest, Hungary.

[6]ELKH-ELTE Space Research Group, Budapest, Hungary.

[7]Department of Physics and Langmuir Laboratory, New Mexico Institute of Mining and Technology, Socorro, NM, USA.

[8]Graduate Program in Electrical Engineering, Federal University of Pará, Belem, Brazil.

[9]HeartMath Institute, Boulder Creek, CA, USA.

[10]British Geological Survey, Edinburgh, UK.

[11]Advanced Environmental Monitoring (AEM), Maryland, USA.

[12]Department of Physics, University of New Brunswick, Fredericton, NB, Canada.

[13]State Institution National Antarctic Scientific Center of Ukraine, Kyiv, Ukraine.

[14]Institute of Electronics, AGH University of Science and Technology, Krakow, Poland.

[15]Department of Physics, University of Alberta, Edmonton, Canada.

[16]Institute of Geophysics, Polish Academy of Sciences, Warsaw, Poland.

[17]Institute of Solar-Terrestrial Physics SB RAS, Irkutsk, Russia.

[18]Sodankylä Geophysical Observatory, University of Oulu, Sodankylä, Finland.

[19]Indian Institute of Geomagnetism, Navi Mumbai, India.

[20]Vaisala, Louisville, CO, USA.

[21]Department of Physics, School of Science, University of Bahrain, Bahrain.

[22]Institute of Radio Astronomy, National Academy of Sciences of Ukraine, Kharkiv, Ukraine.

Corresponding author: Tamás Bozóki (Bozoki.Tamas@epss.hu)

Key Points

- Daily average SR intensity is a quasi-global invariant quantity that shows good agreement with global daily stroke rates and thunder hours.
- Global lightning activity can vary by a factor of 2-3 on a 3-5 day timescale which could be attributed to cold air outbreaks.
- Currently available technology does not allow the detailed quantitative evaluation of lightning activity on continental scales.

Abstract

The importance of lightning has long been recognized from the point of view of climate-related phenomena. However, the detailed investigation of lightning on global scales is currently hindered by the incomplete and spatially uneven detection efficiency of ground-based global lightning detection networks and by the restricted spatio-temporal coverage of satellite observations. We are developing different methods for investigating global lightning activity based on Schumann resonance (SR) measurements. SRs are global electromagnetic resonances of the Earth-ionosphere cavity maintained by the vertical component of lightning. Since charge separation in thunderstorms is gravity-driven, charge is typically separated vertically in thunderclouds, so every lightning flash contributes to the measured SR field. This circumstance makes SR measurements very suitable for climate-related investigations. In this study, 19 days of global lightning activity in January 2019 are analyzed based on SR intensity records from 18 SR stations and the results are compared with independent lightning observations provided by ground-based (WWLLN, GLD360 and ENTLN) and satellite-based (GLM, LIS/OTD) global lightning detection. Daily average SR intensity records from different stations exhibit strong similarity in the investigated time interval. The inferred intensity of global lightning activity varies by a factor of 2-3 on the time scale of 3-5 days which we attribute to continental-scale temperature changes related to cold air outbreaks from polar regions. While our results demonstrate that the SR phenomenon is a powerful tool to investigate global lightning, it is also clear that currently available technology limits the detailed quantitative evaluation of lightning activity on continental scales.

Plain Language Summary

Lightning is recognized as a climate variable indicating the changing climate of the Earth. Surface temperature changes on the order of 1 ^{o}C can result in a significant change in lightning frequency. Lightning activity is monitored on a global scale by satellites and by ground-based global lightning detection networks. However, the detection efficiency of these available technologies is limited which restricts the investigation of global lightning activity especially on the day-to-day time scale. In this study, we propose an alternative method to monitor day-to-day changes in global lightning activity based on Schumann resonance (SR) measurements and thus we compare SR-based observations with available global lightning monitoring techniques. We show that the overall intensity of global lightning activity can vary considerably (by a factor of 2-3) within a few days, further motivating our efforts to monitor

such changes. It is also clear from our study that new methods are needed to quantitatively characterize continental-scale lightning activity.

1. Introduction

Global lightning activity is known as an essential indicator of global climate and has the potential to reveal important consequences of climate change (Aich et al., 2018). The main argument behind this statement is the nonlinear relation between lightning activity and surface temperature (Williams, 1992). Temperature perturbations on the order of 1 ^{o}C have pronounced local effects on cloud electrification which can result in a significant change in lightning frequency (up to 10% per 1 ^{o}C) depending on the time scale investigated (Williams, 2005). A dramatic increase (up to 300%) of lightning has been revealed at Arctic latitudes which correlates well with the global temperature anomaly indicating a temperature enhancement from 0.65°C to 0.95°C in the Arctic region (Holzworth et al., 2021). However, there is some uncertainty in this result, which is related to the time-dependent detection efficiency of the applied lightning detection network. In a more global context it has been shown that the global lightning record from the Lightning Imaging Sensor (LIS) shows statistically flat behavior over the 2002–2013 period, which is often termed a 'hiatus' in global warming with flat temperature trend (Williams et al., 2019). Recently, the radiated energy of global lightning activity has been described using a rigorous quantum physics framework, which is expected to help better understand the impact of climate change on global lightning and the Earth's atmosphere in general (Füllekrug, 2021a).

Lightning is not only an indicator but also a driver of climate change by producing strong greenhouse gasses (Price et al., 1997; Schumann & Huntrieser, 2007). A strong correlation has also been found between convective intensity and upper tropospheric water vapor, one further key element of Earth's climate, and lightning is related to convective intensity (Plotnik et al., 2021; Price, 2000). This result underlines that thunderstorms play an important role in the global redistribution of water, a key mediator of both short and long wavelength radiation (Williams, 2005). All these aspects motivate efforts to monitor the long-term characteristics of lightning on local, regional, and global scales, including the stroke occurrence rate, the average charge transfer, the flash intensity and extent, as well as the distribution of thunderstorm-affected areas, lightning hotspots and lightning superbolts (e.g., Albrecht et al., 2016; Beirle et al., 2014; Blakeslee et al., 2014; Blakeslee et al., 2020; Boldi et al., 2018; Cecil et al., 2015; Chronis & Koshak, 2017; Holzworth et al., 2019; Lyons et al., 2020; Peterson et al., 2021).

About 50 lightning flashes occur every second at any given time on Earth (Christian et al., 2003) and this rate can vary by as much as 10-20% on different time scales (Aich et al., 2018; Albrecht et al., 2016; Cecil et al., 2014; Williams, 2020). Optical detection carried out by satellites provides one way to study lightning activity on global scales. Lightning detection from Low Earth Orbit (LEO), like the Lightning Imaging Sensor (LIS) onboard the Tropical Rainfall Measuring Mission (TRMM, 1997-2015, Christian et al., 2003) and the International Space Station (ISS, February 2017-present, Blakeslee et al., 2020), lays the foundations for essential statistical studies. The limitation of this technique is that continuous monitoring of a specific thunderstorm area is not possible as lightning strokes outside the suborbital swath are not detected. On the other hand, lightning detection from Geostationary Earth Orbit (GEO), like the Geostationary Lightning Mapper (GLM) instrument onboard the GOES-R series satellites (Goodman et al., 2013) and the Lightning Mapping Imager (LMI) instrument onboard the FengYun-4A satellite (Yang et al., 2017), provides continuous lightning monitoring for a given longitudinal sector. Although the appearance of these satellite-based methods represent a major advance for lightning detection on global scales, the current lack of global coverage (i.e., all longitudinal sectors) and the general limitations of optical lightning detection (e.g., the dependence on cloud thickness and time of the day) call for alternative approaches.

Ground-based monitoring of global lightning activity represents another possibility for lightning research, with simultaneous world-wide coverage and with less elaborate and costly infrastructure. Global ground-based lightning monitoring utilizes the electromagnetic (EM) signal emitted by lightning for detection. As the power radiated by lightning peaks in the Very Low Frequency (VLF, 3–30 kHz) band (Wait, 1970) global lightning activity can be monitored with a network of VLF receivers. Such networks require hundreds of VLF (or broadband) receiver stations to achieve global coverage. The World Wide Lightning Location Network (http://wwlln.net) is a collaboration among over 50 universities and institutions for providing lightning locations based on this technique. Currently, two additional global lightning detection networks are in operation: the Global Lightning Detection Network (GLD360) of Vaisala and Earth Networks Total Lightning Network (ENTLN).

The detection efficiency of global lightning detection networks is a key issue for their applicability in climate research (Virts et al., 2013). However, the detection efficiencies are generally unknown, partly because of the lack of a reliable reference dataset (Burgesser, 2017) and partly because of the confidentiality of this information for commercially-operated networks. Even the locations of receiver stations are known only for the research-oriented WWLLN network. For a one year period between November 2014 and October 2015, the absolute global detection efficiency of GLD360, ENTLN and WWLLN has been estimated to be 59.8%, 56.8% and 7.9%, respectively, based on Bayesian analysis (Bitzer & Burchfield, 2016). However, for relatively strong discharges these values are significantly higher (for example in the case of the WWLLN this detection efficiency is about 50% based on Hutchins et al., 2012). It is to be emphasized that these detection efficiencies are spatially uneven (see e.g., Hutchins et al., 2012; Marchand et al., 2019; Rudlosky et al., 2015), restricts detailed investigation of lightning on global scales and prevents the detailed quantitative comparison of lightning activity on continental scales on time scales ranging from the diurnal to the interannual. One important example of this limitation is that lightning activity in Africa is usually underestimated by these networks as compared to Earth's other two main lightning 'chimneys' in the Americas and Asia (Williams & Mareev, 2014). The lower number of receiver stations in the African region is one of the plausible explanations for this observation (Williams & Mareev, 2014). From all these aspects it can be concluded that despite substantial interest in investigating global lightning activity for meteorological/climatological purposes, this endeavor is considerably limited by the vagaries of detection efficiency with available lightning monitoring technologies.

The attenuation of EM waves in the lowest part (<100 Hz) of the Extremely Low Frequency (ELF, 3 Hz - 3 kHz) band (in the range of 0.2-0.5 dB/Mm; Chapman et al., 1966; Wait, 1970) is substantially smaller than in the VLF band (in the range of 1-10 dB/Mm; Barr et al., 2000; Hutchins et al., 2013; Taylor, 1960). This fact enables the investigation of global lightning activity with a much lower number of receiver stations (1–20). In the ELF band lightning-radiated EM waves travel a number of times around the globe in the waveguide formed by the Earth's surface and the lower ionosphere before losing most of their energy. The constructive interference of the EM waves propagating in opposite directions (direct and antipodal waves) creates global EM resonances called Schumann resonances (SRs) which can be observed at ~8, ~14, ~20, etc. Hz (Balser & Wagner, 1960; Galejs, 1972; Madden & Thompson, 1965; Nickolaenko & Hayakawa, 2002; Price, 2016; Schumann, 1952; Wait, 1970). While SR frequencies can be used to deduce temporal changes in the global displacement and migration of lightning activity (e.g., Koloskov et al., 2020; Sátori, 1996; Sátori & Zieger, 1999; Sátori & Zieger, 2003) as well as in the areal compactness of global lightning (Nickolaenko & Rabinowicz, 1995; Nickolaenko et al., 1998; Sátori & Zieger, 2003), SR intensities are known to indicate the overall intensity of global lightning activity (Boldi et al., 2018; Clayton & Polk, 1977; Heckman et al., 1998; Nickolaenko & Hayakawa, 2002; Sentman & Fraser, 1991). Several works have already shown that variations of SRs are consistent with climatological lightning distributions provided by satellite-based lightning detection (e.g., Boldi et al., 2018; Füllekrug, 2021b; Sátori et al., 2009). SRs represent the transverse magnetic (TM) resonance mode of the Earth-ionosphere cavity resonator, which can be excited by vertical lightning discharges (Jackson, 1975). Since the ice-based process of charge separation in thunderstorms is gravity-driven, charge is basically separated vertically in a thundercloud, so every lightning flash in the atmosphere (intracloud and cloud-to-ground alike) is guaranteed to contribute to the SR intensity. This makes SR observations well-suited for climate-related studies (see e.g., Sátori, 1996; Sátori et al., 2009; Williams, 2020; Williams et al., 2021).

The AC global electric circuit as manifest in Schumann resonances is a technically-involved electromagnetic phenomenon (Madden & Thompson, 1965), standing in sharp contrast with the simpler treatment of the DC global electric circuit, which is modeled as a giant spherical capacitor (Haldoupis et al., 2017) characterized by a single scalar: the ionospheric potential (Markson, 2007). The long-standing quest for an equivalent scalar quantity for SRs was initiated by Sentman & Fraser (1991) as the sum of magnetic modal intensities. The aim here was to average out the complicated source-receiver distance effects to approximate the global behavior by introducing a globally invariant SR-based quantity. Their three-decade-old suggestion is tested in the present work in an unprecedented way.

The understanding of the response of global lightning to temperature on short time scales has been stymied historically by the traditional monthly resolution of datasets on global surface air temperature (e.g., Hansen & Lebedeff, 1987). In this study, the global land surface temperature anomaly and lightning activity are analyzed with daily resolution. This investigation has the potential to reveal important variability of the climate system that could change over time as a result of climate change. On this time scale, global effects of cold air outbreaks, when very cold air masses are transported from polar to mid- and low-latitudes, become readily apparent, as will be elaborated on below.

Episodic intrusions of cold air from high latitudes into warmer air at low latitudes have been extensively investigated under the names 'cold surges', 'polar air outbreaks', 'cold air outbreaks' and 'freeze events', and provide a plausible explanation for global temperature perturbations lasting for one to several days. In extreme events, the colder equator-moving air can extend across the equator into the opposite hemisphere and impact the local tropical temperature at the level of 1C. An excellent summary can be found in Hastenrath (1996). Such events may originate in either northern (Hartjenstein & Block, 1991) or southern hemispheres, but the literature is more abundant in studies in southern hemisphere winter (Kousky, 1979; Lanfredi & Camargo, 2018; Lupo et al., 2001; Marengo et al., 1997; Prince & Evans, 2018). The reason for this imbalanced attention may arise because the Antarctic winter air is colder than Arctic air, and because the protection of coffee plantations during freeze events in Brazil is of substantial economic interest (Marengo et al., 1997). The longitudinally-confined nature of the polar outbreaks results in lower-latitude impacts that are sometimes confined to individual continental chimneys (America, Africa, Southeast Asia), with corresponding collections of events in Prince & Evans (2018), Crossett & Metz (2017), Murakami (1979), respectively, or to broader impacts affecting multiple chimneys (Metz et al., 2013) as the equatorward-moving cold air also advects eastward.

In this study, we analyze global lightning activity from 13 to 31 January 2019 based on SR intensity records from 18 SR stations around the globe and compare the results with lightning observations provided by independent ground-based (WWLLN, GLD360 and ENTLN) and satellite-based (GLM, LIS/OTD) global lightning detection. The main motivation of this study is a) to show that global lightning can vary substantially on a day-to-day basis and b) to demonstrate that SR measurements are very well suited to monitor and investigate these day-to-day variations. It is to be highlighted that this is the first study to analyze such a large number of SR stations simultaneously. We will show that summing the first three modes of the two magnetic field components and averaging these values on a daily basis results in a quantity that exhibits very similar (but not exactly identical) behavior at all SR stations studied, and is therefore called a quasi-global invariant.

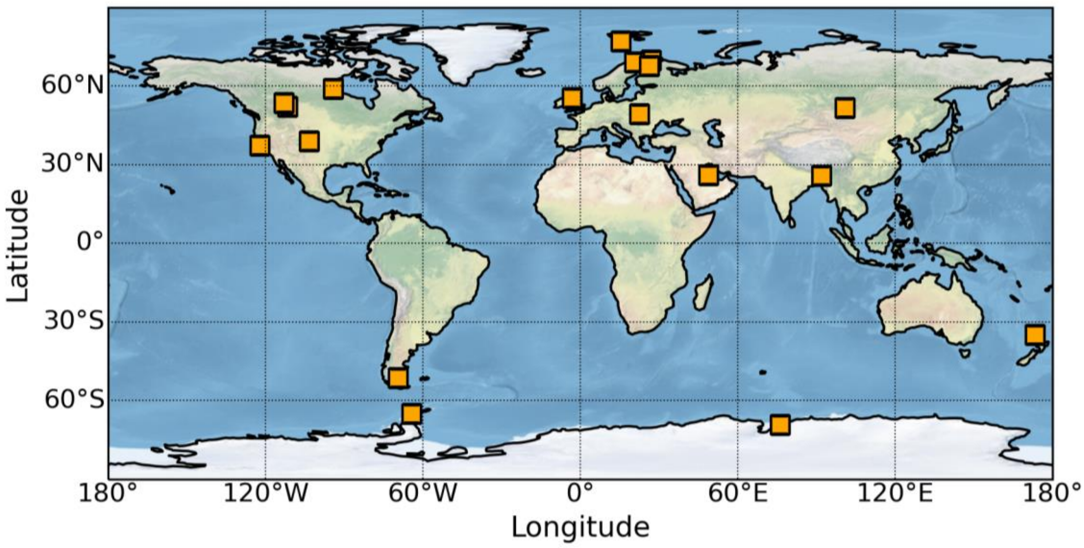

Figure 1. Map showing the locations of the 18 SR stations used in the study (marked by orange squares).

2. Data and Methods

2.1. Data on Schumann Resonances

The most important information about the 18 SR stations used in this study are listed in Table 1 and their locations are shown in Fig.1. All the stations are equipped with a pair of induction coil magnetometers that are in most cases aligned with the local geographical meridian and perpendicular to it, except at the Fort Churchill (FCHU), Ministik Lake (MSTK) and Mondy (MND) stations where they are oriented along the geomagnetic north-south (NS) and east-west (EW) directions. The ALB, BOU, HOF and NOR stations are operated by the Heartmath Institute (https://www.heartmath.org/gci/) and are used mainly to study the relationship between humans and our electromagnetic environment (e.g., Timofejeva et al., 2021). The BRT and SHI stations are operated by the Indian Institute of Geomagnetism. The low resolution (64 Hz) data from the low latitude SHI station in India have been used to study ionospheric Alfven resonances (IAR) (e.g., Adhitya et al., 2022) while high resolution (256 Hz) data from the Antarctic BRT station have been used to examine finer structures of electromagnetic ion cyclotron (EMIC) waves (e.g., Kakad et al., 2018; Upadhyay et al., 2022). The ESK station is operated by the British Geological Survey and is dedicated to study SRs and ionospheric Alfven resonances (see e.g., Beggan & Musur, 2018; Musur & Beggan, 2019). The HRN station in Svalbard is maintained by the Institute of Geophysics (Polish Academy of Sciences) and has been used to study SRs for almost two decades (e.g., Neska et al., 2019; Sátori et al., 2007). The MND station belongs to the Institute of Solar-Terrestrial Physics (Russian Academy of Sciences). This station has been recently used to investigate globally observable ELF-transients (Marchuk et al., 2022). The VRN station in Antarctica is operated by the Institute of Radio Astronomy (National Academy of Sciences of Ukraine) and is one of the most extensively used stations in SR research (e.g., Koloskov et al., 2020; Koloskov et al., 2022; Sátori et al., 2016). The FCHU and MSTK stations are part of the CARISMA network (carisma.ca, Mann et al., 2008) operated by the University of Alberta. These stations are mainly used to study EMIC/Pc1 waves (Kim et al., 2018; Matsuda et al., 2021). The HUG, HYL and PAT stations belong to the World ELF Radiolocation Array (WERA, http://www.oa.uj.edu.pl/elf/index/projects3.htm, Kulak et al., 2014) operated by the Krakow ELF group. The primary objective of WERA is to radiolocate and characterize strong lightning discharges from around the world (e.g., Marchenko et al., 2020; Mlynarczyk et al., 2017; Strumlik et al., 2021). The KEV, KIL and SOD stations are part of the Finnish pulsation magnetometer chain (https://www.sgo.fi/Data/Pulsation/pulDescr.php) operated by the Sodankylä Geophysical Observatory, University of Oulu. Characterisation of EMIC/Pc1 waves and monitoring Alfven resonances is also a primary goal of this network. In a recent study ALB, BOU, HRN and ESK stations have been utilized to investigate the evolution of continental-scale lightning activity on the timescale of the El Niño–Southern Oscillation (ENSO) (Williams et al., 2021). In another work long-term changes in the properties of the Earth-ionosphere waveguide have been analyzed based on the HRN, ESK, SHI and VRN stations (Bozóki et al., 2021). The analysed period (13-31 January 2019) was selected based on the availability of data from all the stations listed. The only exception is Mondy (MND) from where data are available only in the 15-30 January period.

Table 1 Detailed information on the 18 SR stations used in the study.

Station	Code	Country	Latitude (°N)	Longitude (°E)	Sampling (Hz)
Alberta	ALB	Canada	51.89	-111.47	130.2
Bharati	BRT	Antarctica	-69.41	76.19	256
Boulder Creek	BOU	USA	37.19	-122.12	130.2
Eskdalemuir	ESK	UK	55.29	-3.17	100
Fort Churchill	FCHU	Canada	58.76	-94.08	100
Hofuf	HOF	Saudi Arabia	25.94	48.95	130.2
Hornsund	HRN	Svalbard	77.0	15.6	100
Hugo	HUG	USA	38.89	-103.40	887.8
Hylaty	HYL	Poland	49.19	22.55	887.8
Kevo	KEV	Finland	69.75	27.02	250
Kilpisjarvi	KIL	Finland	69.05	20.79	250
Ministik Lake	MSTK	Canada	53.35	-112.97	100
Mondy	MND	Russia	51.6	100.9	64
Northland	NOR	New Zealand	-35.11	173.49	130.2
Patagonia	PAT	Argentina	-51.59	-69.32	887.8
Shillong	SHI	India	25.6	91.9	64
Sodankyla	SOD	Finland	67.43	26.39	250
Vernadsky	VRN	Antarctica	-65.25	-64.25	320

In the following we describe how to obtain the quasi-global invariant quantity from SR measurements. All the raw SR time series were processed in the same way. First, standardized one-hour time series have been generated from raw data files with different formats. In this step, the measured data were filtered using a finite impulse response (FIR) bandpass filter, which also corrected for the amplitude response of the recording systems. For the Heartmath stations (ALB, BOU, HOF, NOR), the amplitude-response function is flat in the SR band, so no correction was applied. For the stations of the Finnish pulsation magnetometer chain (KEV, KIL, SOD), the amplitude response of the measuring system is not known. For the WERA stations (HUG, HYL, PAT) a color noise (1/f type noise) appears in the measurements (see Fig.2 in Mlynarczyk et al., 2017) which cannot be corrected by the amplitude response function, so no correction was applied. Based on the bandwidths of the measuring systems and the available information about the amplitude responses, the bandpasses of the FIR filters has been chosen to be 2-45 Hz for the ALB, BOU, ESK, HOF, HRN, HUG, HYL, NOR, PAT and VRN stations, 2-31 Hz for the FCHU, MSTK, KEV, KIL and SOD stations, and 2-30 Hz for the BRT, MND and SHI stations. For the three stations with geomagnetic orientation (FCHU, MSTK, MND) a digital antenna rotation has been applied (Mlynarczyk et al., 2015) when generating the standardized time series in order to transform the records to the geographical main directions.

As the next step in the overall procedure, sanitized power spectral density (PSD) spectra were calculated from the standardized time series based on Welch's method (Welch, 1967). This method estimates the PSD by dividing the data into overlapping segments, determining the PSD of each segment and averaging them. First, spikes larger than 100 pT (in absolute value) were replaced by nans ("not a number"-s) in the time domain to minimize the aliasing effect of regional lightning activity (Tatsis et al., 2021) and exceptionally intense lightning strokes known as Q-bursts (Guha et al., 2017). PSD spectrograms (dynamic spectra) were calculated with a window length (depending on the sampling frequency of the actual stations) corresponding to ~0.1 Hz frequency resolution and a half-window-length overlap. This step unifies the PSD spectra obtained from stations operating at different sampling frequencies. We refer to one column of the spectrogram (dynamic spectrum) which corresponds to the PSD spectrum of one window as a "spectral segment". Those windows that contained nans resulted in spectral segments with only nans (usually around 1-2% of all the spectral segments). Next, narrowband, anthropogenic noises (Salinas et al., 2022), identified manually for each station, have been removed from the spectra. One further sanitation step has been applied based on the spectral power content (SPC) (the sum of PSD values) (Guha et al., 2017) in the lowest part of the spectrum (<6 Hz) and in the SR band (6-30 Hz or 6-40 Hz depending on the bandwidth of the station) where segments with SPC greater than the average plus one standard deviation (either below 6 Hz or in the SR band) has been removed. This is a strict criterion but its application results in very clear SR spectrograms characteristic of "background" lightning activity, without the influence of nearby or remote but very powerful lightning. If the number of removed spectral segments was greater than 40%, then that hour was labeled "bad quality data" and not used (this number of removed spectral segments is usually between 20% and 30%). Finally, average resonance peaks have been fitted for stations with narrower/wider bandwidth, respectively. Finally, we summed the intensities of the first three resonance modes (~8 Hz, ~14 Hz, ~20 Hz) as the main contributor from each magnetic coil to the quasi-global invariant quantity of central interest in this work.

2.2. Independent Lightning Observations

The characteristics of global lightning activity as inferred from the values of the magnetic intensity for the 19-day long period of 13-31 January 2019 are compared with independent lightning observations provided by three global, ground-based lightning monitoring networks: the World Wide Lightning Location Network (WWLLN), the Global Lightning Detection Network (GLD360) and the Earth Networks Total Lightning Network (ENTLN) as well as satellite-based optical lightning observations carried out by the LIS/OTD instruments (climatological) and the Geostationary Lightning Mapper (GLM) onboard the GOES-16 and GOES-17 satellites. The latter provides lightning locations for the American longitudinal sector (i.e., the Western Hemisphere). Two kinds of WWLLN lightning data (RelocB and AE) are available for the study. Algorithms yielding RelocB and AE data are much the same, based on sferic identification in VLF waveforms, determination of times of group arrivals, finding matching pairs, and event localizing. RelocB is the 'official' WWLLN data product. The criteria and parametrizing of the sferic identification, and selection of stations taken into account in pairing has been somewhat altered in a newer code (AE), where - semi heuristic - lightning energies are also involved as additional derivatives. Energy is not provided by the RelocB. The altered AE algorithm resulted in minor differences between the two sets of identified lightning. LIS/OTD observations are taken from the 0.5°x0.5° High Resolution Monthly Climatology (HRMC) dataset (Cecil, 2006). It is to be noted that the ground-based/satellite-based observations provide strokes/flashes, respectively.

2.3. Earth Networks Thunder Hour

Earth Networks recently released Thunder Hours, a new data product that is available and freely accessible for climate research purposes from 2014 to date (DiGangi et al., 2022). Earth Networks Thunder Hour is defined simply as an hour during which thunder can be heard in a particular area (in this case, within a 15 km radius) and is simulated using total lightning data from a combined set of ENTLN- and WWLLN-detected lightning locations called Earth Networks Global Lightning Detection Network (ENGLN). The dataset is available in 0.05^{o}x0.05^{o} spatial resolution and one of its main strengths is that it helps to reduce the influence of detection efficiency on the lightning climatology (DiGangi et al., 2022). In this study we calculate the total daily number of thunder hours for the whole globe and for the three main lightning chimneys and compare them with the SR-based quasi-global invariant quantity.

2.4. Daily Land-Surface Temperature

Berkeley Earth provides an experimental temperature time series with daily resolution (http://berkeleyearth.lbl.gov/auto/Global/Complete_TAVG_daily.txt) which is called the daily land-surface average anomaly and is produced by the Berkeley Earth averaging method described on their website. In this dataset land-surface temperatures are reported as anomalies relative to the January 1951 - December 1980 average. Although the product is said to be preliminary and could be significantly revised in the future, we consider it a roughly correct indicator of day-to-day changes in the global land temperature.

3. Results

Figure 2 shows the worldwide lightning activity measured by satellites (Fig.2a,b) and by ground-based lightning monitoring networks (Fig.2c,d,e,f). While the LIS/OTD observations show climatological lightning activity for January, all other observations cover the period 13-31 January 2019. In the investigated time interval lightning activity is concentrated in the tropical land regions and in the land areas of the Southern Hemisphere, corresponding to the three main lightning "chimney" regions: the Maritime Continent, Africa and South America. This is consistent with the expectation based on solar heating that in Northern Hemispheric winter months global lightning shifts into the Southern Hemisphere (Christian et al., 2003). The LIS/OTD January climatology (Fig.2a) indicates that the African chimney (with largest activity in the Congo basin) is predominant among the three main chimney regions in January. This expectation is not clearly met in the GLD360 (Fig.2c) and ENTLN (Fig.2d) lightning maps and it is definitely not true in case of the WWLLN observations (Fig.2e,f). Further differences can be identified among GLD360, ENTLN and WWLLN lightning maps. Strong lightning activity is detected by GLD360 and by WWLLN in the eastern equatorial part of Brazil which is less dominant in the ENTLN dataset. On the other hand, ENTLN reports strong lightning activity in the eastern part of South Africa which is less dominant in GLD360 and WWLLN observations. The latter difference between GLD360 and ENTLN could be explained by a higher detection for GLD360 in the Congo basin than that of ENTLN (note the different color scales of the maps). The lightning maps also demonstrate that the WWLLN is unique in the sense that it locates intense lightning events globally, far from ground network coverage (e.g., eastward and westward from Central America). The distribution of GLM detected lightning flashes in South America shows the closest similarity with GLD360 observations. These various observations may be summarized with one important conclusion: detection efficiency is a key unknown in the intercomparison of different lightning observations.

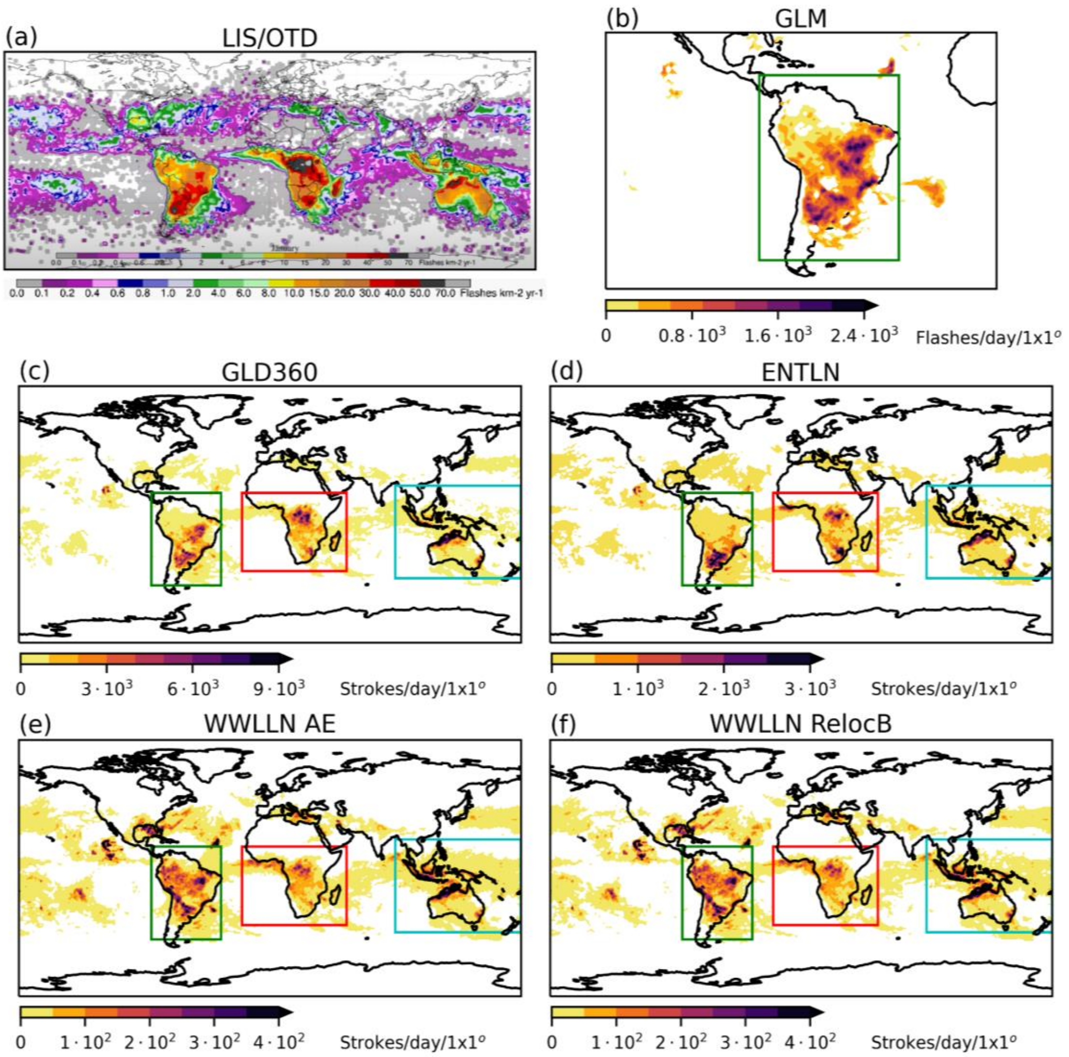

Figure 2. Lightning activity in the 13-31 January 2019 period as seen by different lightning detection methods (except in panel **a** which shows climatological lightning activity for January based on HRMC LIS/OTD observations (Cecil, 2006)). Green (South America), red (Africa) and blue (Maritime Continent) rectangles show those parts of the lightning maps for which stroke/flash numbers and thunder hours are summarized in the chimney-by-chimney analysis (Fig.5 and Fig.6c,d). Note that the upper limits of the color scales are different for the different lightning detection methods.

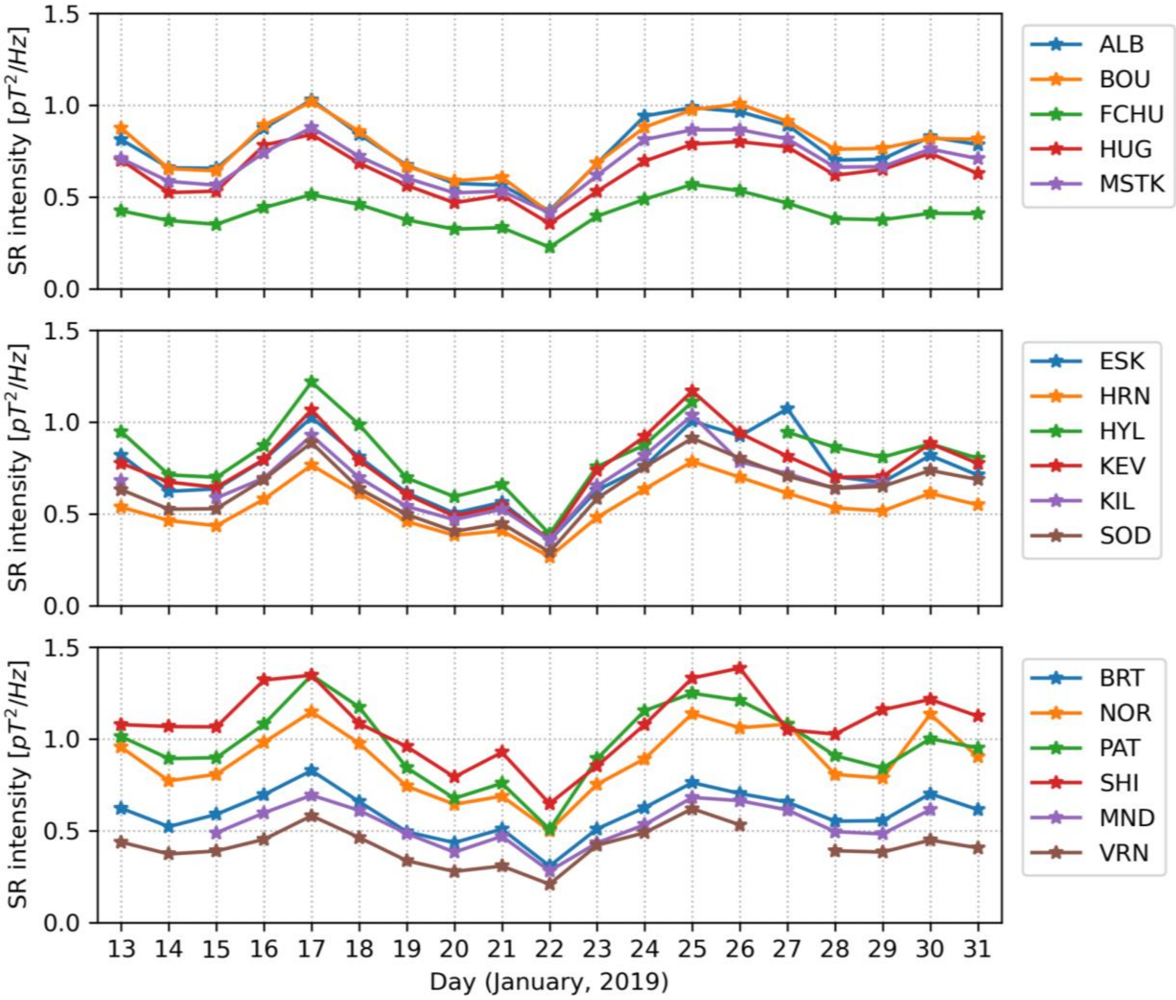

Figure 3. Daily average SR intensity values (the sum of the first three modes and of the two magnetic field components) in the 13-31 January 2019 period. The top panel shows SR intensity records from North America, the middle panel SR intensity records from Europe while the bottom panel SR intensity records from other parts of the globe. A similar behavior of all station records is noted over the 19-day time scale.

Figure 3 shows daily average SR intensity records from 18 stations around the globe. The daily average values are calculated as the sum of the first three SR modes and of the two magnetic field components, in units of pT^2/Hz. The striking similarity between the different records is unambiguous. All of them show a clear maximum on the 17th of January, a well-pronounced minimum on the 22nd of January and a second maximum on the 25-26 of January. A third, smaller maximum can be seen on the 30th of January. SR intensity drops by more than a factor of 2 from 17 to 22 January, i.e. in just 5 days. Given the accumulated evidence that lightning intensity is proportional to SR intensity (e.g., Boldi et al., 2018; Clayton & Polk, 1977), the finding suggests a similar reduction in the overall intensity of global lightning activity over this time interval. The possible origins of this large variation on the day-to-day timescale will be addressed in the Discussion. While the general trends in the different records are very similar, the apparent differences in absolute levels are probably connected to the different distances between the active lightning source regions and the SR stations. Furthermore, some problems probably also arise with the absolute calibration of the magnetic measurements. That is the reason why we call the daily average SR intensity a *quasi-global* invariant quantity. This could possibly be sorted out by similar intercomparisons in different seasons characterized by different source geometries.

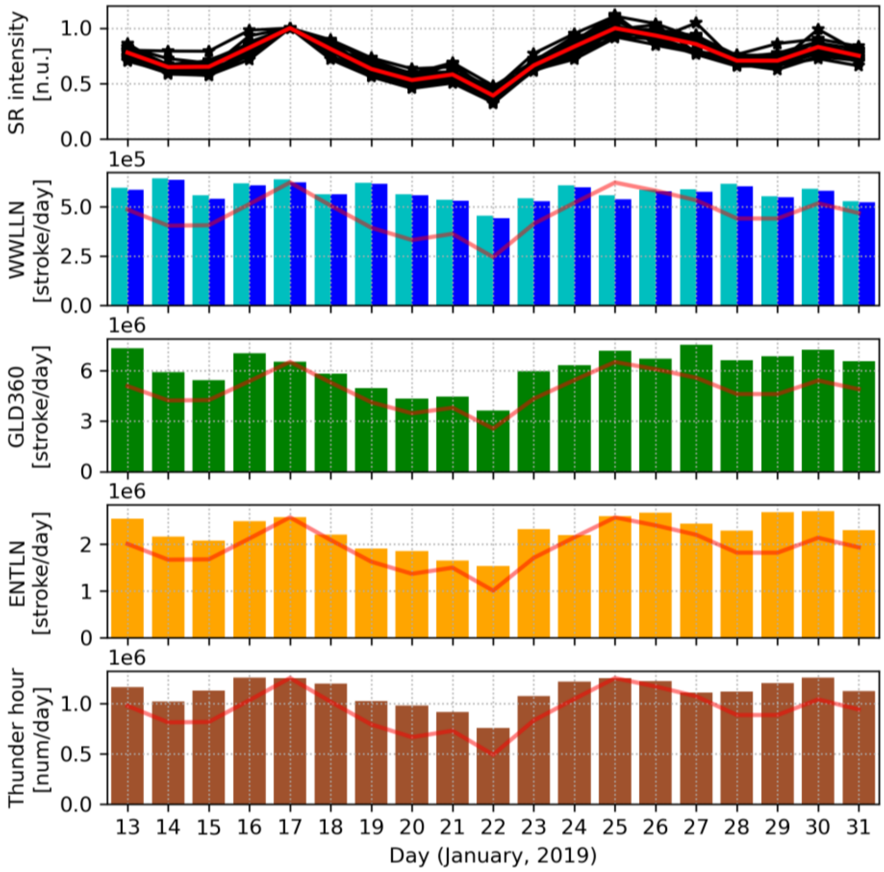

Figure 4. Comparison of normalized daily average SR intensity records (in normalized units) with the total (global) daily stroke rates provided by independent lightning observations (WWLLN, GLD360, ENTLN) and with the total daily numbers of Earth Networks Thunder Hours. In the top subplot black curves correspond to different SR stations while the red curve shows the average of all records. The scaled version of the latter curve is also shown in the other four subplots. In the second row WWLLN RelocB/AE data are shown in cyan/blue, respectively.

Further comparisons with other measures of global lightning activity over the same 19 day interval are shown in Fig.4. In the top row all the daily average SR intensity records from Fig.3 are displayed but now by applying a normalization with respect to the daily average value on the 17th of January. This step reduces the source-observer distance dependence and calibration problems and makes the high degree of similarity among the different SR intensity records even more obvious. The second, third, fourth and fifth subpanels show the total (global) daily stroke rates provided by the WWLLN (cyan/blue: RelocB/AE), GLD360, and ENTLN as well as the total daily numbers of Earth Networks Thunder Hours. Note that the limits of the y axis are different for the different lightning detection networks. GLD360 reports about 3 times more events than ENTLN and more than 10 times more events than WWLLN. GLD360 and ENTLN data follow the general trend of the normalized average SR intensity record quite well (correlation coefficients are: 0.81 and 0.83 for GLD360 and ENTLN, respectively) and are both superior in this aspect in comparison with WWLLN (correlation coefficients are: 0.52 and 0.48 for WWLLN RelocB and AE, respectively). WWLLN RelocB provides about 15% higher daily stroke rates than WWLLN AE but the general trends (day-to-day variations) are very similar in the two datasets. Since the WWLLN is most efficient at detecting high amplitude lightning, this observation may suggest that the day-to-day variation of high amplitude lightning is different from the day-to-day variation of the "average" lightning that maintains SRs. The total daily numbers of Earth Networks Thunder Hours yield the best correlation coefficient with the average SR intensity record: 0.89.

It is to be noted that the relative variation of SR intensity records is considerably larger (more than a factor of 2) than that of other lightning records (usually less than a factor of 2). In Table 2 percentage variations of SR intensity are compared with the different lightning observations for those selected days when SR intensity shows the two largest maxima on 17 and 25 January as well as a pronounced minimum on 22 January. The largest percentage increase/decrease appears in the average SR intensity and in the GLM records (Table 2) while the smallest increase/decrease in the WWLLN observations.

Table 2. Percentage changes in average SR intensity and in other lightning observations between 17 and 22 January as well as between 22 and 25 January.

January days	SR	WWLLN AE	WWLLN RelocB	GLD360	ENTLN	Thunder hour	GLM
17 → 22	-61 %	-29 %	-29 %	-44 %	-40 %	-40%	-52 %
22 → 25	+113 %	+36 %	+34 %	+74 %	+43 %	+61%	+107%

Figure 5 represents the contributions of individual continental chimneys to the global variations in Figs. 3 and 4. It presents SR intensity and independent lightning observations from day to day for the three main lightning chimney regions (the Maritime Continent, Africa and South America) in the time intervals (Maritime Continent: 7-11 UT, Africa: 13-17 UT, South America: 18-22 UT) when lightning activity is the strongest in the respective chimney region (local afternoon hours). The top row shows normalized SR intensity records for selected stations and field components for which the corresponding wave propagation path crosses the actual chimney region (see the Supplementary material for details). On each day SR magnetic intensities are averaged for the first three modes in pT^2/Hz in the time intervals indicated in the top of the figure. The day-to-day changes are different for the three main chimney regions although clear similarities can also be observed between pairs of records. There is again a very high similarity among the SR intensity records from different stations confirming the global representativeness of SR intensity in any time intervals (hours) of a day.

In case of the independent lightning observations (second, third, fourth and fifth rows of Fig.5), lightning strokes and thunder hours are summarized for the same time intervals as SR intensities within the color-coded rectangles marked in Fig.2. We suppose that these areas contain the main lightning sources for SR intensity. Figure 5 reveals that it is the diminishment of African lightning activity on 22 January that causes the minimum in global lightning activity identified in Fig.4. South American lightning activity is also reduced on this day but this reduction starts a few days earlier. The high correlation between GLD360 and ENTLN for the total (global) daily stroke rates (0.93) drops considerably in this chimney-by-chimney analysis (Maritime Continent: 0.78, Africa: 0.79, South America: 0.34). For the Maritime Continent and South America, it is GLD360 that yields the highest correlation with the average SR intensity record (0.49 and 0.67, respectively), while for Africa the ENTLN stroke rates perform the best in this aspect (0.77). This means that thunder hours are not as representative for SRs on the chimney-scale as they were in the global analysis (Fig.4).

We are also interested in the chimney ranking, i.e. the relative strength of the three main lightning chimney regions. Such information on a day-to-day basis may be important for synoptic meteorology and forecasting. This information is lost in the presented SR intensity records when they are normalized with respect to the average value on the 17th of January. Another problem is that SR intensities strongly depend on the source-observer distance, which hinders us from directly utilizing SR intensity records from multiple stations to infer the chimney ranking. We would need to apply an inversion approach to extract this information from the SR records (see e.g., Prácser et al., 2019; Nelson, 1967; Shvets & Hayakawa, 2011) but this step is out of the scope of the present study. Therefore, we turn to independent lightning observations to investigate the question of chimney ranking. WWLLN indicates that the African chimney has the lowest activity of the three, contrary to the findings of prior studies (e.g., Brooks, 1925), but the African chimney also has the fewest WWLLN receivers of the three. Therefore, this inconsistency could be rooted in detection efficiency issues. The GLD360 and ENTLN daily stroke rates do not show characteristic differences between the three main chimney regions (Fig.5, horizontal black lines). The Asian/African/South American chimneys are the most powerful on 10/5/4 days in the GLD360 dataset and on 7/9/3 days in the ENTLN dataset, respectively. On the other hand, thunder hours show the clear dominance of the African lightning chimney in accordance with LIS/OTD lightning climatology (Fig.2a). From all these results it is clear that the available lightning monitoring techniques do not provide a consistent and reliable ranking of lightning activity in the three main chimney regions.

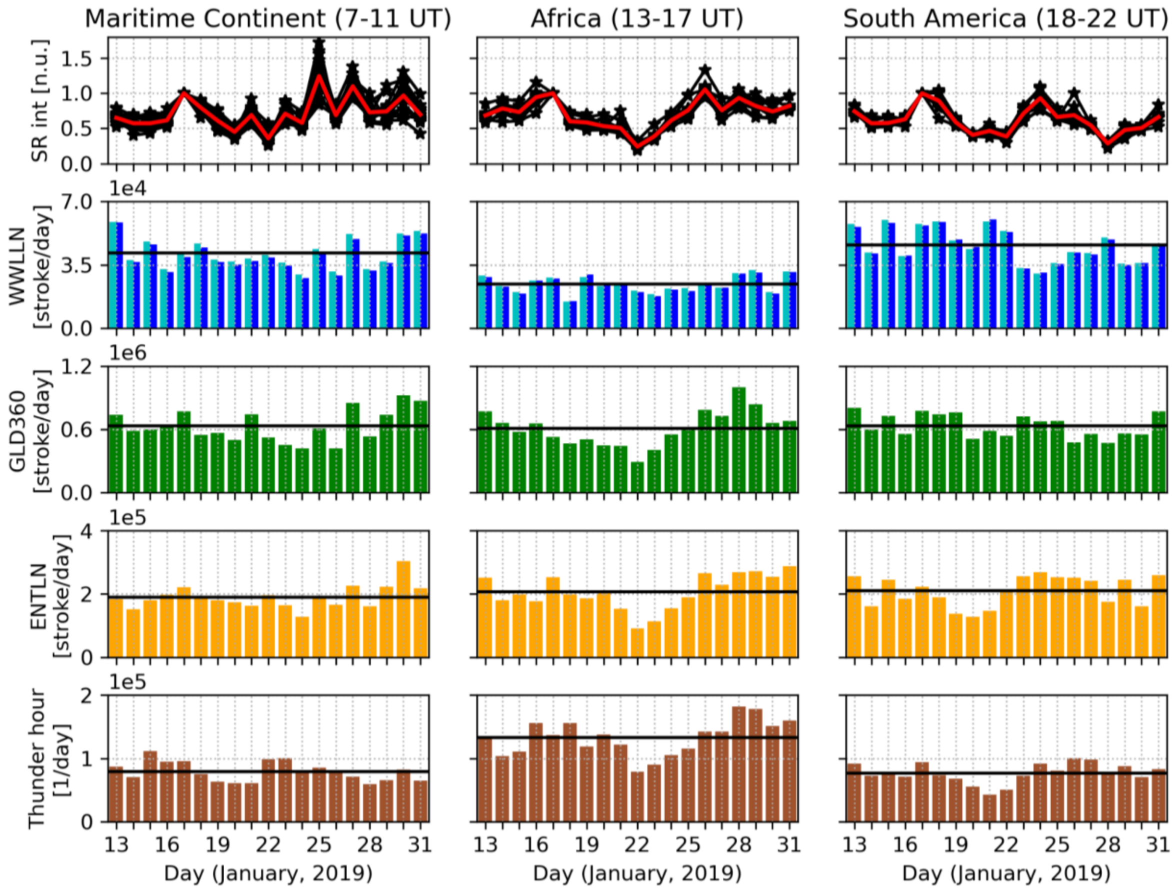

Figure 5. Chimney-by-chimney comparison of normalized average SR intensity records (in normalized units) with stroke rates and thunder hours provided by independent lightning observations (see text for more details). In the top row, black curves correspond to magnetic intensity integrations for different sets of SR stations while the red curve shows the average of all SR stations in each grouping. In the second, third, fourth and fifth rows, horizontal black lines indicate the mean values of the various plotted quantities.

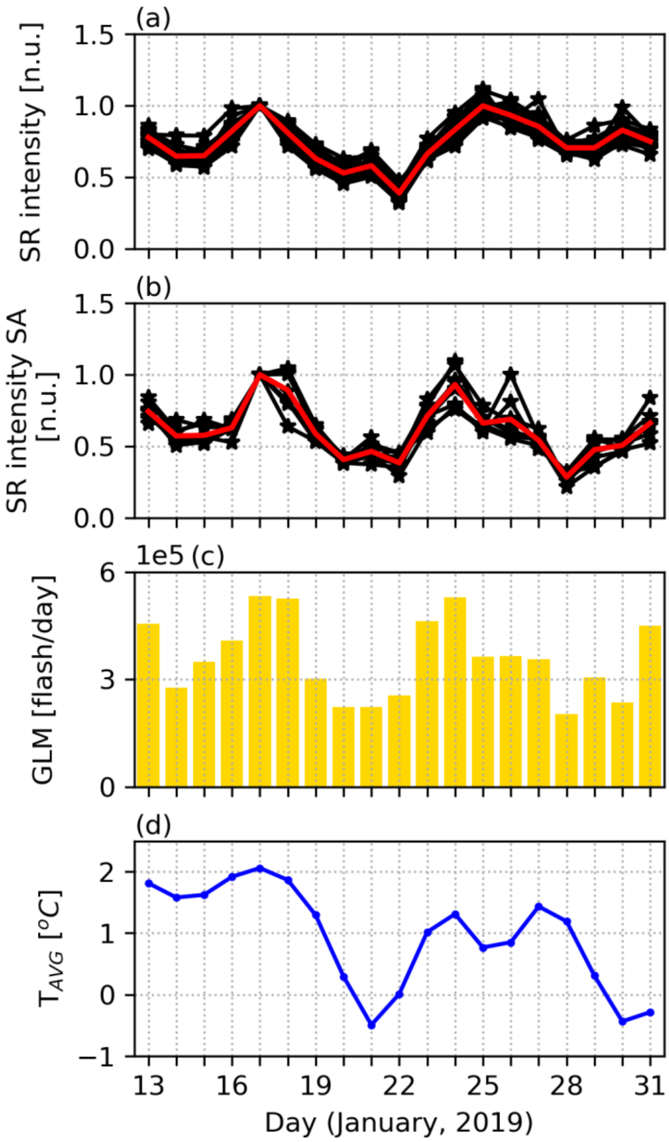

Figure 6. Comparison of (a) normalized daily average SR intensity records (in normalized units) with (b) the normalized average SR intensity records of South America (in normalized units), (c) daily flash rates provided by the GLM instrument and (d) the Berkeley Earth daily land-surface temperature average (TAVG) anomaly. GLM-detected lightning flashes had been summarized within the green rectangle (representing South America) marked in Fig.2.

Figure 6 shows the comparison of normalized daily average SR intensity records for the globe (Fig.6a) with the normalized average SR intensity records of South America (Fig.6b), GLM daily flash rates (Fig.6c) and the Berkeley Earth daily temperature average (TAVG) values (Fig.6d). The daily TAVG anomaly time series clearly shows a similar trend to the daily average SR intensity records i.e., a maximum on 17 January, a minimum on 21 January (this minimum is on 22 January in the SR data) and a second maximum on 24 January (this maximum is on 25 January in the SR data). The inferred overall diminishment in global temperature over four days is ~2.5 C^o, a substantial change. This observation strongly suggests a thermodynamic origin of the global lightning variations indicated by the SR intensity records. Such substantial changes in global temperature are possibly linked to cold air outbreaks

(Hastenrath, 1996) when a large amount of very cold air mass is transported from polar latitudes into warmer regions at low latitudes. There is an excellent agreement between the average SR intensity record corresponding to South America (Fig.6b) and the daily flash rates provided by GLM (Fig.6c). It is noteworthy that the GLM flash counts, representing the entire Western Hemisphere, decline by approximately a factor of two from Jan 17 to Jan 22, in concert with the global quasi-invariant quantity (Fig.6a). The correlation coefficient between these two datasets is 0.93, which is much larger than the correlation between GLM and GLD360/ENTLN (0.69 and 0.63, respectively). This result can be regarded as a validation of our approach for producing quasi-global invariant SR intensity records characterizing individual chimneys.

4. Discussion

Although lightning is recognized now as an essential climate variable by the World Meteorological Organization (WMO) (Aich et al., 2018), the continuous monitoring of global lightning activity on the day-to-day timescale is severely limited as indicated by the apparently inconsistent global lightning distributions presented in Fig.2. Satellite observations do not provide global coverage on this timescale while the detection efficiency of available global ground-based lightning monitoring networks is limited, spatially uneven, and generally unknown (just as the location of the receiving stations is not freely accessible in the case of the GLD360 and ENTLN networks). Moreover, the detection efficiency of these networks is not stable but varies from day to day depending on the actual lightning distribution (see Fig. 2 in Bitzer & Burchfield, 2016). Another important manifestation of this limitation is that even simple questions such as “which of the main lightning chimney regions was the strongest on a given day” currently cannot be answered unambiguously (Fig.5). However, it should also be pointed out that the available technologies are constantly improving: for example ENTLN has undergone a very significant processor upgrade since the investigated period (Zhu et al., 2022), and geostationary lightning monitoring will soon be available for the European longitude sector as well (Holmlund et al., 2021).

Of the three global ground-based lightning detection networks studied here, the WWLLN network is clearly the least representative globally, and this is mainly related to its low detection efficiency in Africa (Fig.5) (Williams & Mareev, 2014). With GLD360 reporting three times as many events as ENTLN (Fig.4) and showing better agreement with GLM data (Fig.2), it is likely that GLD360 was the most reliable and globally representative ground-based lightning detection network during the investigated period. However, based on our results, Earth Networks Thunder Hours (based on the ENTLN lightning dataset) is a very promising quantity for investigating day-to-day variations of global lightning activity (Fig.4).

Schumann resonance measurements offer a cost-effective way to monitor global lightning activity. However, SR intensity values do not provide direct information on the distribution of lightning activity at sub-continental scale. For this purpose we plan to use in the future an inversion algorithm aimed to infer the location and intensity of global lightning based on SR measurements (Dyrda et al., 2014; Nelson, 1967; Prácser et al., 2019; Prácser et al., 2022; Shvets et al., 2010; Shvets et al., 2011; Shvets & Hayakawa, 2011; Williams & Mareev, 2014). The main difficulty in interpreting SR measurements is the complicated source-receiver distance dependence of the resonance field (see e.g., Nickolaenko & Hayakawa, 2002). It is a long-standing goal of SR research to derive a scalar quantity, a SR-based “geoelectric index”, that characterizes the overall intensity of global lightning activity by eliminating this source-receiver distance effect (Holzworth & Volland, 1986; Sentman & Fraser, 1991). Our work followed the long recommended strategy of averaging the intensity of the two field components and as many resonance modes as possible (Sentman & Fraser, 1991; Nieckarz et al., 2009).

Several studies have previously analyzed SR intensity data from multiple stations (e.g., Bozóki et al., 2021; Füllekrug & Fraser-Smith, 1996; Price, 2000; Sentman & Fraser, 1991; Williams & Sátori, 2004; Williams et al., 2021), but to the best of our knowledge, this is the first work that shows for many stations that summing the first three modes of the two magnetic components and averaging these values on a daily basis results in a quasi-global invariant quantity. This quantity shows a very good agreement with total (global) daily stroke rates provided by independent lightning observations and with the total daily numbers of Earth Networks Thunder Hours (Fig.4).

Our group sees great potential in comparing different geophysical parameters with the introduced quasi-global invariant quantity on the day-to-day time scale. The latter can be considered as an indicator of the day-to-day changes in the low-latitude atmospheric updraft, and thus it seems appropriate to investigate whether the upper layers of the atmosphere show considerable variability similar to the very significant day-to-day variability in global lightning activity. The work by Price (2000) can be regarded as such an approach where the author used an SR-based quantity as indicator for day-to-day changes in upper tropospheric water vapor. We also see it as an intriguing question whether there is a parameter (e.g., fluctuations in electron density) specific to the low-latitude ionosphere that correlates with the SR-based quantity we introduced.

At this point, some apparent limitations of the introduced SR-based quantity also need to be discussed. One major limitation is that in its current form, the quasi-global invariant quantity is not really suitable for studying longer time periods. The main reason for this statement is that on longer time scales, the source-observer distance effect associated with the seasonal north-south migration of global lightning activity causes significant changes in SR intensity (Nickolaenko et al., 1998) that are not corrected in the current form of the quasi-global invariant quantity. Further investigations are needed to clarify this likely difficulty, but it is recommended that the quantity introduced should only be used within a one-month period. Changes in the properties of the Earth-ionosphere cavity, i.e. the propagation conditions of ELF waves on the even longer interannual time scale (Bozóki et al., 2021), are another challenge that needs to be addressed in the future. Shorter timescale changes in the properties of the Earth-ionosphere cavity associated with space weather, for example connected with energetic electron precipitation (Bozóki et al., 2021), with geomagnetic storms (Pazos et al., 2019; Salinas et al., 2016), with solar proton events (Roldugin et al., 2003; Schlegel and Füllekrug, 1999), and with the solar rotation (Füllekrug & Fraser-Smith, 1996) can also bias the SR-based characterization of global lightning activity. However, in the present study, where a time interval close to the minimum of solar activity was investigated, there is no clear evidence of a significant space weather effect based on comparisons with independent lightning observations.

Observations in this study of global lightning on daily time scales have raised the interest in cold air outbreaks, a mechanism causing a global change in mean surface air temperature on the same time scale. We showed indications for a northern hemisphere winter event, with influence in both the American and the African chimney. The chimney-by-chimney information on lightning activity presented in Fig.5 suggests that the cold air outbreak initiated in the American longitudinal sector and then shifted eastwards and reached the African longitudes. This scenario is supported by surface skin temperature observations (not shown here) indicating that the cold outbreak first impacted the American chimney and then affected the African chimney as the temperature perturbation moved both equatorward and eastward.

In this study, our interest lies primarily in thermodynamic impacts on global lightning. However, given the recognized influence of aerosol on lightning activity (e.g., Williams, 2020), it should be noted that cold air outbreaks can also deliver cleaner polar air to lower latitude locations (e.g., Liu et al., 2019). The satellite-based method of estimating CCN concentration at cloud base height (Rosenfeld et al., 2016) was used to look for reductions in pollution linked with the equatorward motion of polar air in America and Africa, but no obvious signatures were identified.

5. Conclusions

In this paper we showed that by summing the intensity of the first three Schumann resonance (SR) modes of the two magnetic components and by averaging these values on a daily basis, a quasi-global invariant quantity can be obtained that can be used to investigate day-to-day changes in global lightning activity, supporting the earlier suggestion by Sentman & Fraser (1991). This quantity revealed significant variability in the overall intensity of global lightning activity that can occur within a few days and is likely explained by large-scale changes in land-surface temperatures related to cold air outbreaks. Independent global lightning datasets showed good agreement with the variations of the quasi-global invariant quantity. However, for the three main lightning chimneys on Earth the agreement among different lightning observations (including the SR invariant) is significantly worse, which underlines the need for improving the available observation methods and calculation techniques in this respect. An inversion algorithm that could infer the distribution and intensity of global lightning activity based on SR measurements would be very valuable to fill this important gap in our knowledge.

Acknowledgement

This work was supported by the National Research, Development, and Innovation Office, Hungary-NKFIH, project numbers K138824 and FK135115. The work of T. Bozóki was supported by the ÚNKP-21-3 New National Excellence Program of the Ministry for Innovation and Technology from the source of the National Research, Development and Innovation Fund. The authors thank I.R. Mann, D.K. Milling and the rest of the CARISMA team for data. CARISMA is operated by the University of Alberta, funded by the Canadian Space Agency. The authors wish to thank the World Wide Lightning Location Network (http://wwlln.net), a collaboration among over 50 universities and institutions, for providing the lightning location data used in this study. The contribution of E. Williams and Y. Liu was supported by a grant from the US National Science Foundation (Grant # 6942697). A. Potapov's contribution was supported by the project of the RF Ministry of Education and Science, and the data from obs. Mondy were obtained using the equipment of Center of Common Use "Angara" http://ckp-rf.ru/ckp/3056. Measurements at Vernadsky station were funded by “State Special-Purpose Research Program in Antarctica for 2011-2023” MES of Ukraine.

Data Availability Statement

Thunder hour data provided by Earth Networks, in collaboration with WWLLN, are available at http://thunderhours.earthnetworks.com. LIS/OTD data are available online (https://ghrc.nsstc.nasa.gov/pub/lis/climatology/) from the NASA EOSDIS Global Hydrology Resource Center Distributed Active Archive Center Huntsville, Alabama, U.S.A. GLM data for this study were obtained through https://console.cloud.google.com/storage/browser/gcp-public-data-goes-16. The Berkeley Earth daily land-surface temperature anomaly record is available at http://berkeleyearth.org/data/. Eskdalemuir induction coil data are collected by the British Geological Survey and are available at https://www.bgs.ac.uk/services/ngdc/accessions/index.html#item131926. ENTLN/GLD360 data are available for research purposes from Earth Networks/Vaisala upon request. The WWLLN data are available at a nominal cost from http://wwlln.net. Normalized daily average Schumann resonance (SR) intensity data are available at: https://doi.org/10.5281/zenodo.7555111

References

Adhitya, P., Nosé, M., Bulusu, J., Vichare, G., & Sinha, A.K. (2022). Observation of ionospheric Alfven resonator with double spectral resonance structures at low latitude station, Shillong (dipoleL=1.08). *Earth Planets Space*, **74**, 169. https://doi.org/10.1186/s40623-022-01730-2

Aich, V., Holzworth, R., Goodman, G., Price, C., & Williams, E. (2018). Lightning: A New Essential Climate Variable. *EOS*, **99**. https://eos.org/science-updates/lightning-a-new-essential-climate-variable

Albrecht, R.I., Goodman, S.J., Buechler, D.E., Blakeslee, R.J., & Christian, H.J. (2016). Where are the lightning hotspots on Earth? *Bull. Am. Meteorol. Soc.*, **97**(11), 2,051–2,068. https://doi.org/10.1175/BAMS-D-14-00193.1

Balser, M., & Wagner, C.A. (1960). Observation of Earth-ionosphere cavity resonances. *Nature*, **188**(4751), 638–641. https://doi.org/10.1038/188638a0

Barr, R., Llanwyn Jones, D., & Rodger, C.J. (2000). ELF and VLF radio waves. *J. Atmos. Sol. Terr. Phys.*, **62**(17–18), 1689–1718. https://doi.org/10.1016/S1364-6826(00)00121-8

Beggan, C.D., & Musur, M. (2018). Observation of ionospheric Alfvén resonances at 1–30 Hz and their superposition with the Schumann resonances. *J. Geophys. Res.: Space Phys.*, **123**(5), 4202– 4214. https://doi.org/10.1029/2018JA025264

Beirle, S., Koshak, W., Blakeslee, R., & Wagner, T. (2014). Global patterns of lightning properties derived by OTD and LIS. *Nat. Hazards Earth Syst. Sci.*, **14**(10), 2715–2726. https://doi.org/10.5194/nhess-14-2715-2014

Bitzer, P.M., & Burchfield, J.C. (2016). Bayesian techniques to analyze and merge lightning locating system data. *Geophys. Res. Lett.*, **43**(24), 12,605– 12,613. https://doi.org/10.1002/2016GL071951

Blakeslee, R.J., Lang, T.J., Koshak, W.J., Buechler, D., Gatlin, P., Mach, D.M., et al. (2020). Three Years of the Lightning Imaging Sensor Onboard the International Space Station: Expanded Global Coverage and Enhanced Applications. *J. Geophys. Res. Atmos.*, **125**(16). https://doi.org/10.1029/2020JD032918

Blakeslee, R.J., Mach, D.M., Bateman, M.G., & Bailey, J.C. (2014). Seasonal variations in the lightning diurnal cycle and implications for the global electric circuit. *Atmos. Res.*, **135-136**, 228–243. https://doi.org/10.1016/j.atmosres.2012.09.023

Boldi, R., Williams, E., & Guha, A. (2018). Determination of the global-average charge moment of a lightning flash using Schumann resonances and the LIS/OTD lightning data. *J. Geophys. Res. Atmos.*, **123**(1), 108–123. https://doi.org/10.1002/2017JD027050

Bozóki, T., Sátori, G., Williams, E., Mironova, I., Steinbach, P., Bland E.C., et al. (2021). Solar Cycle-Modulated Deformation of the Earth–Ionosphere Cavity. *Front. Earth Sci.*, **9**. https://doi.org/10.3389/feart.2021.689127

Brooks, C.E.P. (1925). *The distribution of thunderstorms over the globe*. Geophys. Mem. London, 24, 147–64.

Burgesser, R.E. (2017). Assessment of the world wide lightning location network (WWLLN) detection efficiency by comparison to the lightning imaging sensor (LIS). *Q. J. R. Meteorolog. Soc.*, **143**(708), 2809–2817. https://doi.org/10.1002/qj.3129

Cecil, D. J., Buechler, D.E., & Blakeslee, R.J. (2014). Gridded lightning climatology from TRMM-LIS and OTD: Dataset description. *Atmos. Res.*, **135-136**, 404–414. https://doi.org/10.1016/j.atmosres.2012.06.028

Cecil, D.J. (2006). LIS/OTD 0.5 Degree High Resolution Monthly Climatology (HRMC). http://dx.doi.org/10.5067/LIS/LIS-OTD/DATA303

Cecil, D.J., Buechler, D.E., & Blakeslee, R.J. (2015). TRMM LIS Climatology of Thunderstorm Occurrence and Conditional Lightning Flash Rates. *J. Clim.*, **28**(16), 6536–6547. https://doi.org/10.1175/JCLI-D-15-0124.1

Chapman, F.W., Llanwyn Jones, D., Todd, J.D.W., & Challinor, R.A. (1966). Observation on the propagation constant of the Earth-ionosphere waveguide in the frequency band 8 kc/s to 16 kc/s. *Radio Sci.*, **1**(11), 1273–1282. https://doi.org/10.1002/rds19661111273

Christian, H.J., Blakeslee, R.J., Boccippio, D.J., Boeck, W.L., Buechler, D.E., Driscoll, K.T., et al. (2003). Global frequency and distribution of lightning as observed from space by the optical transient detector. *J. Geophys. Res.*, **108**(D1), ACL 4-1–ACL 4-15. https://doi.org/10.1029/2002JD002347

Chronis, T., & Koshak, W.J. (2017). Diurnal Variation of TRMM/LIS Lightning Flash Radiances. *Bull. Am. Meteorol. Soc.*, **98**(7), 1453–1470. https://doi.org/10.1175/BAMS-D-16-0041.1

Clayton, M., & Polk, C. (1977). Diurnal Variation and Absolute Intensity of Worldwide Lightning Activity, September 1970 to May 1971. In H. Dolezalek & R. Reiter (Eds.), *Electrical Processes in Atmospheres* (pp. 440). Darmstadt, West Germany: Verlag.

Crossett, C.C., & Metz, N.D. (2017). A Climatological Study of Extreme Cold Surges along the African Highlands. *J. App. Met. Clim.*, **56**, 1731–1738. https://doi.org/10.1175/JAMC-D-15-0191.1

DiGangi, E.A., Stock, M., & Lapierre, J. (2022). Thunder Hours: How Old Methods Offer New Insights into Thunderstorm Climatology. *Bull. Am. Meteorol. Soc.*, **103**(2), E548–E569. https://doi.org/10.1175/BAMS-D-20-0198.1

Dyrda, M., Kulak, A., Mlynarczyk, J., Ostrowski, M., Kubisz, J., Michalec, A., & Nieckarz, Z. (2014). Application of the Schumann resonance spectral decomposition in characterizing the main African thunderstorm center. *J. Geophys. Res. Atmos.*, **119**(23), 13,338–13,349. https://doi.org/10.1002/2014JD022613

Füllekrug, M., & Fraser-Smith, A.C. (1996). Further evidence for a global correlation of the Earth-ionosphere cavity resonances. *Geophys. Res. Lett.*, **23**(20), 2773-2776. https://doi.org/10.1029/96GL02612

Füllekrug, M. (2021a). Global lightning quanta. *J. Geophys. Res. Atmos.*, **126**(9). https://doi.org/10.1029/2020JD033201

Füllekrug, M. (2021b). Simulation of Earth-ionosphere cavity resonances with lightning flashes reported by OTD/LIS. *J. Geophys. Res. Atmos.*, 126(24). https://doi.org/10.1029/2021JD035721

Galejs, J. (1972). *Terrestrial Propagation of Long Electromagnetic Waves*. New York: Pergamon.

Goodman, S.J., Blakeslee, R.J., Koshak, W.J., Mach, D., Bailey, J., Buechler, D., et al. (2013). The GOES-R geostationary lightning mapper (GLM). *Atmos. Res.*, **125-126**, 34–49. https://doi.org/10.1016/j.atmosres.2013.01.006

Guha, A., Williams, E., Boldi, R., Sátori, G., Nagy, T., Bór, J., et al. (2017). Aliasing of the Schumann Resonance Background Signal by Sprite-Associated Q-Bursts. *J. Atmos. Solar-Terrestrial Phys.*, **165-166**, 25–37. https://doi.org/10.1016/j.jastp.2017.11.003

Haldoupis, C., Rycroft, M., Williams, E., & Price, C. (2017). Is the "Earth-ionosphere capacitor" a valid component in the atmospheric global electric circuit? *J. Atmos. Sol. Terr. Phys.*, **164**, 127–131. https://doi.org/10.1016/j.jastp.2017.08.012

Hansen, J., & Lebedeff, S. (1987). Global trends of measured surface air temperature. *J. Geophys. Res.*, **92**(D11), 13,345–13,372. https://doi.org/10.1029/JD092iD11p13345

Hartjenstein, G.& Block, G.B. (1991). Factors affecting cold-air outbreaks east of the Rocky Mountains. *Mon. Wea. Rev.*, **119**, 2280–2292. https://doi.org/10.1175/1520-0493(1991)119<2280:FACAOE>2.0.CO;2

Hastenrath, S., 'Cold surges', Section 7.9 in *Climate Dynamics of the Tropics*, Kluwer Academic Publishers, Reprinted 1996.

Heckman, S., Williams, E., & Boldi, R. (1998). Total global lightning inferred from Schumann resonance measurements. *J. Geophys. Res.*, **103**(D24), 31,775–31,779. https://doi.org/10.1029/98JD02648

Holmlund, K., Grandell, J., Schmetz, J., Stuhlmann, R., Bojkov, B., Munro, R., et al. (2021). Meteosat Third Generation (MTG): Continuation and Innovation of Observations from Geostationary Orbit. *Bull. Am. Meteorol. Soc.*,**102**(5), E990–E1015. https://doi.org/10.1175/BAMS-D-19-0304.1

Holzworth, R.H., Brundell, J.B., McCarthy, M.P., Jacobson, A.R., Rodger, C.J., & Anderson, T.S. (2021). Lightning in the Arctic. *Geophys. Res. Lett.*, **48**(7). https://doi.org/10.1029/2020GL091366

Holzworth, R.H., McCarthy, M.P., Brundell, J.B., Jacobson, A.R., & Rodger, C.J. (2019). Global distribution of superbolts. *J. Geophys. Res. Atmos.*, **124**(17-18), 9,996–10,005. https://doi.org/10.1029/2019JD030975

Holzworth, R., & Volland, H. (1986). Do we need a geoelectric index? *Eos Trans. AGU*, **67**(26), 545–548. https://doi.org/10.1029/EO067i026p00545-01

Hutchins, M.L., Holzworth, R.H., Brundell, J.B., & Rodger, C.J. (2012). Relative detection efficiency of the World Wide Lightning Location Network. *Radio Sci.*, **47**(6). https://doi.org/10.1029/2012RS005049

Hutchins, M.L., Jacobson, A.R., Holzworth, R.H., & Brundell, J. B. (2013). Azimuthal dependence of VLF propagation. *J. Geophys. Res.: Space Phys.*, **118**(9), 5808–5812. https://doi.org/10.1002/jgra.50533

Jackson, J.D. (1975). *Classical Electrodynamics*, second ed. Wiley, New York, NY. https://cds.cern.ch/record/100964

Kakad, B., Omura, Y., Kakad, A., Upadhyay, A., & Sinha, A.K. (2018). Characteristics of subpacket structures in ground EMIC wave observations. *J. Geophys. Res.: Space Phys.*, **123**(10), 8358–8376. https://doi.org/10.1029/2018JA025473

Kim, H., Hwang, J., Park, J., Miyashita, Y., Shiokawa, K., Mann, I.R., Raita, T., & Lee, J. (2018). Large-scale ducting of Pc1 pulsations observed by Swarm satellites and multiple ground networks. *Geophys. Res. Lett.*, **45**(23), 12,703–12,712. https://doi.org/10.1029/2018GL080693

Koloskov, A.V., Nickolaenko, A.P., Yampolsky, Y.M., Yu, C., Budanov, O.V., & Budanov, O.V. (2020). Variations of Global Thunderstorm Activity Derived from the Long-Term Schumann Resonance Monitoring in the Antarctic and in the Arctic. *J. Atmos. Sol. Terr. Phys.*, **201**, 105231. https://doi.org/10.1016/j.jastp.2020.105231

Koloskov, O.V., Nickolaenko, A.P., Yampolski, Y.M., & Budanov, O.V. (2022). Electromagnetic seasons in Schumann resonance records. *J. Geophys. Res. Atmos.*, **127**(17), e2022JD036582. https://doi.org/10.1029/2022JD036582

Kousky, V.E. (1979). Frontal influences on Northeast Brazil. *Mon. Wea. Rev.*, **107**, 1140–1153. http://dx.doi.org/10.1175/1520-0493(1979)107<1140:FIONB>2.0.CO;2

Kulak, A., Kubisz, J., Klucjasz, S., Michalec, A., Mlynarczyk, J., Nieckarz, Z., et al. (2014). Extremely low frequency electromagnetic field measurements at the Hylaty station and methodology of signal analysis. *Radio Sci.*, **49**(6), 361–370. https://doi.org/10.1002/2014RS005400

Kulak, A., Mlynarczyk, J., Zieba, S., Micek, S., & Nieckarz, Z. (2006). Studies of ELF propagation in the spherical shell cavity using a field decomposition method based on asymmetry of Schumann resonance curves. *J. Geophys. Res.: Space Phys.*, **111**(A10). https://doi.org/10.1029/2005JA011429

Lanfredi, I.S., & de Camargo, R. (2018). Classification of extreme cold incursions over South America. *Weather and Forecasting*, **33**, 1183–1203. https://doi.org/10.1175/WAF-D-17-0159.1

Liu, Q., Chen, G., & Iwasaki, T. (2019). Quantifying the impacts of cold airmass on aerosol concentrations over North China using isentropic analysis. *J. Geophys. Res. Atmos.*, 124(13), 7308–7326. https://doi.org/10.1029/2018JD029367

Lupo, A.R., Nocera, J.J., Bosart, L.F., Hoffman, E.G., & Knight, D.J. (2001). South American Cold Surges: Types, Composites, and Case Studies. *Mon. Weather Rev.*, **129**(5), 1021–1041. https://doi.org/10.1175/1520-0493(2001)129<1021:SACSTC>2.0.CO;2

Lyons, W.A., Bruning, E.C., Warner, T.A., MacGorman, D.R., Edgington, S., Tillier, C., & Mlynarczyk, J. (2020). Megaflashes: Just How Long Can a Lightning Discharge Get? *Bull. Am. Meteorol. Soc.*, **101**(1), E73–E86. https://doi.org/10.1175/BAMS-D-19-0033.1

Madden, T., & Thompson, W. (1965). Low-frequency electromagnetic oscillation of the Earth-ionosphere cavity. *Rev. Geophys.*, **3**(2), 211–254. https://doi.org/10.1029/RG003i002p00211

Mann, I. R., Milling, D.K., Rae, I.J., Ozeke, L.G., Kale, A., Kale, Z.C., et al. (2008). The upgraded CARISMA magnetometer array in the THEMIS era. *Space Sci. Rev.*, **141**, 413–451. https://doi.org/10.1007/s11214-008-9457-6

Marchand, M., Hilburn, K., & Miller, S. D. (2019). Geostationary lightning mapper and Earth networks lightning detection over the contiguous United States and dependence on flash characteristics. *J. Geophys. Res. Atmos.*, **124**(21), 11552–11567. https://doi.org/10.1029/2019JD031039

Marchenko, V., Mlynarczyk, J., Ostrowski, M., Kulak, A., Senchenko, O., Kubisz, J., et al. (2021). Study of a TGF associated with an Elve using extremely low frequency electromagnetic waves. *J. Geophys. Res. Atmos.*, **126**(3), e2020JD033070. https://doi.org/10.1029/2020JD033070

Marchuk R.A., Potapov A.S., Mishin V. . (2022). Synchronous globally observable ultrashort-period pulses. *Solar-Terrestrial Physics*, **8**(2), 47–55. https://doi.org/10.12737/stp-82202207

Marengo, J., Cornejo, A., Satyamurty, P., Nobre, C., & Sea, W. (1997). Cold Surges in Tropical and Extratropical South America: The Strong Event in June 1994. *Mon. Weather Rev.*, **125**(11), 2759–2786. https://doi.org/10.1175/1520-0493(1997)125<2759:CSITAE>2.0.CO;2

Markson, R. (2007). The Global Circuit Intensity: Its Measurement and Variation over the Last 50 Years. *Bull. Am. Meteorol. Soc.*, **88**(2), 223–242. https://doi.org/10.1175/BAMS-88-2-223

Matsuda, S., Miyoshi, Y., Kasahara, Y., Blum, L., Colpitts, C., Asamura, K., et al. (2021). Multipoint measurement of fine-structured EMIC waves by Arase, Van Allen Probe A, and ground stations. *Geophys. Res. Lett.*, **48**(23), e2021GL096488. https://doi.org/10.1029/2021GL096488

Metz, N.D., Archambault, H.M., Shrock, A.F., Galarneau, T. J. Jr., Bosart, L.F. (2013). A Comparison of South American and African Preferential Pathways for Extreme Cold. *Mon. Weather Rev.*, **141**, 2066–2086. https://doi.org/10.1175/MWR-D-12-00202.1

Mlynarczyk, J., Bór, J., Kulak, A., Popek, M., & Kubisz, J. (2015). An unusual sequence of sprites followed by a secondary TLE: An analysis of ELF radio measurements and optical observations. *J. Geophys. Res.: Space Phys.*, **120**(3), 2241–2254. https://doi.org/10.1002/2014JA020780

Mlynarczyk, J., Kulak, A., & Salvador, J. (2017). The accuracy of radio direction finding in the extremely low frequency range. *Radio Sci.*, **52**(10), 1245– 1252. https://doi.org/10.1002/2017RS006370

Murakami, T. (1979). Winter monsoonal surges over East and Southeast Asia. *J. Met. Soc., Japan*, **57**, 133–158.

Musur, M. A., & Beggan, C. D. (2019). Seasonal and Solar Cycle Variation of Schumann Resonance Intensity and Frequency at Eskdalemuir Observatory, UK. Sun and Geosphere, 14(1). https://doi.org/10.31401/SunGeo.2019.01.11

Nelson, P.H. (1967). *Ionospheric perturbations and Schumann resonance data*. Project NR-371-401. (PhD dissertation), Cambridge, MA:Geophysics Laboratory, Massachusetts Institute of Technology.

Neska, M., Czubak, P., & Reda, J. (2019). Schumann Resonance Monitoring in Hornsund (Spitsbergen) and Suwałki (Poland). Publs. Inst. Geophys. P.A.S. 425, 41–45. https://doi.org/10.25171/InstGeoph_PAS_Publs-2019-008

Nickolaenko, A.P., & Hayakawa, M. (2002). *Resonances in the Earth-Ionosphere Cavity*. Dordrecht: Kluwer.

Nickolaenko, A.P., & Rabinowicz, L.M. (1995). Study of the annual changes of global lightning distribution and frequency variations of the first Schumann resonance mode. *J. Atmos. Terr. Phys.*, **57**(11), 1345–1348. https://doi.org/10.1016/0021-9169(94)00114-4

Nickolaenko, A.P., Sátori, G., Zieger, B., Rabinowicz, L.M., Kudintseva, I.G. (1998). Parameters of global thunderstorm activity deduced from long-term Schumann resonance records. *J. Atmos. Sol. Terr. Phys.*, **60**(3), 387–399. https://doi.org/10.1016/S1364-6826(97)00121-1

Nieckarz, Z., Kułak, A., Zięba, S., Kubicki, M., Michnowski, S., & Barańskiaverage, P. (2009). Comparison of global storm activity rate calculated from Schumann resonance background components to electric field intensity E0Z. *Atmos. Res.*, **91**(2-4), 184–187. https://doi.org/10.1016/j.atmosres.2008.06.006

Pazos, M., Mendoza, B., Sierra, P., Andrade, E., Rodríguez, D., Mendoza, V., et al. (2019). Analysis of the Effects of Geomagnetic Storms in the Schumann Resonance Station Data in Mexico. *J. Atmos. Solar-Terrestrial Phys.*, **193**, 105091. https://doi.org/10.1016/j.jastp.2019.105091

Peterson, M., Mach, D., & Buechler, D. (2021). A global LIS/OTD climatology of lightning Flash Extent Density. *J. Geophys. Res. Atmos.*, **126**(8). https://doi.org/10.1029/2020JD033885

Plotnik, T., Price, C., Saha, J., & Guha, A. (2021). Transport of Water Vapor from Tropical Cyclones to the Upper Troposphere. *Atmosphere*. **12**(11), 1506. https://doi.org/10.3390/atmos12111506

Prácser, E., & Bozóki, T. (2022). On the reliability of the inversion aimed to reconstruct global lightning activity based on Schumann resonance measurements. *J. Atmos. Sol. Terr. Phys.*, **235**, 105892. https://doi.org/10.1016/j.jastp.2022.105892

Prácser, E., Bozóki, T., Sátori, G., Williams, E., Guha, A., & Yu, H. (2019). Reconstruction of Global Lightning Activity Based on Schumann Resonance Measurements: Model Description and Synthetic Tests. *Radio Sci.*, **54**(3), 254–267. https://doi.org/10.1029/2018RS006772

Price, C. (2000). Evidence for a link between global lightning activity and upper tropospheric water vapour. *Nature*, **406**, 290–293. https://doi.org/10.1038/35018543

Price, C. (2016). ELF electromagnetic waves from lightning: The Schumann resonances. *Atmosphere*, **7**(9). https://doi.org/10.3390/atmos7090116

Price, C., Penner, J., & Prather, M. (1997). NOx from lightning: 1. Global distribution based on lightning physics. *J. Geophys. Res.*, **102**(D5), 5929–5941. https://doi.org/10.1029/96JD03504

Prince, K.C., & Evans, C. (2018). A Climatology of Extreme South American Andean Cold Surges. *J. App. Met. Clim.*, **57**, 2297–2315. https://doi.org/10.1175/JAMC-D-18-0146.1

Roldugin, V.C., Maltsev, Y.P., Vasiljev, A.N., Shvets, A.V., & Nikolaenko, A.P. (2003). Changes of Schumann Resonance Parameters During the Solar Proton Event of 14 July 2000. *J. Geophys. Res.: Space Phys.*, **108**(A3). https://doi.org/10.1029/2002JA009495

Rosenfeld, D., Zheng, Y., Hashimshoni, E., Pöhlker, M.L., Jefferson, A., Pöhlker, C. et al. (2016). Satellite retrieval of cloud condensation nuclei concentrations by using clouds as CCN chambers. *PNAS*, **113**(21). https://doi.org/10.1073/pnas.1514044113

Rudlosky, S. D. (2015). Evaluating ENTLN performance relative to TRMM/LIS. *J. Operational Meteor.*, **3**(2), 1120. http://dx.doi.org/10.15191/nwajom.2015.0302

Salinas, A., Toledo-Redondo, S., Navarro, E.A., Fornieles-Callejón, J., and Portí, J.A. (2016). Solar Storm Effects During Saint Patrick's Days in 2013 and 2015 on the Schumann Resonances Measured by the ELF Station at Sierra Nevada (Spain). *J. Geophys. Res. Space Phys.*, **121**(12), 12,234-12,246. https://doi.org/10.1002/2016JA023253

Salinas, A., Rodríguez-Camacho, J., Portí, J., Carrión, M.C., Fornieles-Callejón, J., Toledo-Redondo, S. (2022). Schumann resonance data processing programs and four-year measurements from Sierra Nevada ELF station. Comput. Geosci., **165**, 105148. https://doi.org/10.1016/j.cageo.2022.105148

Sátori, G. (1996). Monitoring Schumann resonances-II. Daily and seasonal frequency variations. *J. Atmos. Terr. Phys.*, **58**(13), 1,483–1,488. http://dx.doi.org/10.1016/0021-9169(95)00146-8

Sátori, G., & Zieger, B. (1999). El Niňo related meridional oscillation of global lightning activity. *Geophys. Res. Lett.*, **26**(10), 1365–1368. https://doi.org/10.1029/1999GL900264

Sátori, G., & Zieger, B. (2003). Areal Variations of the Worldwide Thunderstorm Activity on Different Time Scales as Shown by Schumann Resonances. In: Serge Chauzy, Pierre Laroche (ed.) *Proceeding of the 12th ICAE*, Global Lightning and Climate. Versailles, France, 2003.06.09-2003.06.13. pp. 765-768.

Sátori, G., Williams, E., & Lemperger, I. (2009). Variability of global lightning activity on the ENSO time scale. *Atmos. Res.*, **91**(2-4), 500–507. http://dx.doi.org/10.1016/j.atmosres.2008.06.014

Sátori, G., Neska, M., Williams, E., & Szendrői, J. (2007). Signatures of the day-night asymmetry of the Earth-ionosphere cavity in high time resolution Schumann resonance records. *Radio Sci.*, **42**(2), RS2S10. https://doi.org/10.1029/2006RS003483

Sátori, G., Williams, E., Price, C., Boldi, R., Koloskov, A., Yampolski, Y., et al. (2016). Effects of Energetic Solar Emissions on the Earth-Ionosphere Cavity of Schumann Resonances. *Surv. Geophys.*, **37**, 757–789. https://doi.org/10.1007/s10712-016-9369-z

Schlegel, K., & Füllekrug, M. (1999). Schumann Resonance Parameter Changes during High-Energy Particle Precipitation. *J. Geophys. Res. Space Phys.*, **104**(A5), 10,111–10,118. https://doi.org/10.1029/1999JA900056

Schumann, U., & Huntrieser, H. (2007). The global lightning-induced nitrogen oxides source. *Atmos. Chem. Phys.*, **7**, 3823–3907. https://doi.org/10.5194/acp-7-3823-2007

Schumann, W.O. (1952). Über die strahlungslosen Eigenschwingungen einer leitenden Kugel, die von einer Luftschicht und einer Ionosphärenhülle umgeben ist. *Zeitschrift für Naturforschung*, **7**(2), 149–154. https://doi.org/10.1515/zna-1952-0202

Sentman, D.D., & Fraser, B.J. (1991). Simultaneous observations of Schumann resonances in California and Australia: Evidence for intensity modulation by the local height of the D region. *J. Geophys. Res.*, **96**(A9), 15973–15984. https://doi.org/10.1029/91JA01085

Shvets, A.V., & Hayakawa, M. (2011). Global lightning activity on the basis of inversions of natural ELF electromagnetic data observed at multiple stations around the world. *Surv. Geophys.*, **32**(6), 705–732. https://doi.org/10.1007/s10712-011-9135-1

Shvets, A. V., Hayakawa, M., Sekiguchi, M., & Ando, Y. (2009). Reconstruction of the global lightning distribution from ELF electromagnetic background signals. *J. Atmos. Sol. Terr. Phys.*, **71**(12), 1405–1412. https://doi.org/10.1016/j.jastp.2009.06.008

Shvets, A. V., Hobara, Y., & Hayakawa, M. (2010). Variations of the global lightning distribution revealed from three-station Schumann resonance measurements. *J. Geophys. Res.: Space Phys.*, **115**, A12316. https://doi.org/10.1029/2010JA015851

Strumik, M., Slominski, J., Slominska, E., Mlynarczyk, J., Blecki, J., Haagmans, R., et al. (2021). Experimental evidence of a link between lightning and magnetic field fluctuations in the upper ionosphere observed by Swarm. *Geophys. Res. Lett.*, **48**(4), e2020GL091507. https://doi.org/10.1029/2020GL091507

Tatsis, G., Sakkas, A., Christofilakis, V., Baldoumas, G., Chronopoulos, S.K., Paschalidou, A.K., et al. (2021). Correlation of Local Lightning Activity with Extra Low Frequency Detector for Schumann Resonance Measurements. *Sci. Total Environ.*, **787**, 147671. https://doi.org/10.1016/j.scitotenv.2021.147671

Taylor, W.L. (1960). VLF attenuation for east-west and west-east daytime propagation using atmospherics. *J. Geophys. Res.*, **65**(7), 1933–1938. https://doi.org/10.1029/JZ065i007p01933

Timofejeva, I., McCraty, R., Atkinson, M., Alabdulgader, A.A., Vainoras, A., Landauskas, M., Šiaučiūnaitė, V., Ragulskis, M. (2021). Global Study of Human Heart Rhythm Synchronization with the Earth's Time Varying Magnetic Field. *Appl. Sci.*, **11**, 2935. https://doi.org/10.3390/app11072935

Virts, K.S., Wallace, J.M., Hutchins, M.L., & Holzworth, R.H. (2013). Highlights of a New Ground-Based, Hourly Global Lightning Climatology. *Bull. Am. Meteorol. Soc.*, **94**(9), 1381–1391. https://doi.org/10.1175/BAMS-D-12-00082.1

Wait, J.R. (1970). *Electromagnetic Wave in Stratified Media*. The Institute of Electrical and Electronics Engineers Inc. New York: Oxford University Press Oxford.

Welch, P. (1967). The Use of Fast Fourier Transform for the Estimation of Power Spectra: A Method Based on Time Averaging over Short, Modified Periodograms. *IEEE Trans. Audio Electroacoust.*, **15**(2), 70–73. https://doi.org/10.1109/TAU.1967.1161901

Williams E.R., & Sátori G. (2004). Lightning, thermodynamic and hydrological comparison of two tropical continental chimneys. *J. Atmos. Sol. Terr. Phys.*, **66**, 1213–1231. https://doi.org/10.1016/j.jastp.2004.05.015

Williams, E., Bozóki, T., Sátori, G., Price, C., Steinbach, P., Guha, A., et al. (2021). Evolution of global lightning in the transition from cold to warm phase preceding two super El Niño events. *J. Geophys. Res. Atmos.*, **126**(3). https://doi.org/10.1029/2020JD033526

Williams, E., Guha, A., Boldi, R., Christian, H., & Buechler, D. (2019). Global lightning activity and the hiatus in global warming. *J. Atmos. Sol. Terr. Phys.*, **189**, 27–34. https://doi.org/10.1016/j.jastp.2019.03.011

Williams, E.R. (1992). The Schumann resonance: A global tropical thermometer. *Science*, **256**(5060), 1184–1187. https://doi.org/10.1126/science.256.5060.1184

Williams, E.R. (2005). Lightning and climate: A review. *Atmos. Res.*, **76**(1–4), 272–287. https://doi.org/10.1016/j.atmosres.2004.11.014

Williams, E.R. (2020). Chapter 2: "Lightning and Climate Change" Chapter 2 in book. In A. Piantini (Ed.), *Lightning Interaction with Power Systems*. Stevenage: UK: The Institution of Engineering and Technology.

Williams, E.R., & Mareev, E.A. (2014). Recent progress on the global electrical circuit. *Atmos. Res.*, **135–136**, 208–227. https://doi.org/10.1016/j.atmosres.2013.05.015

Upadhyay, A., Kakad, B., Kakad, A., & Rawat, R. (2022). A statistical study of modulation of electromagnetic ion cyclotron waves observed on ground. *J. Geophys. Res.: Space Phys.*, **127**(8), e2022JA030340. https://doi.org/10.1029/2022JA030340

Yang, J., Zhang, Z., Wei, C., Lu, F., & Guo, Q. (2017). Introducing the New Generation of Chinese Geostationary Weather Satellites, Fengyun-4. *Bull. Am. Meteorol. Soc.*, **98**(8), 1637–1658. https://doi.org/10.1175/BAMS-D-16-0065

Zhu, Y., Stock, M., Lapierre, J., & DiGangi, E. (2022). Upgrades of the Earth Networks Total Lightning Network in 2021. *Remote Sens.*, **14**(9), 2209. https://doi.org/10.3390/rs14092209

JGR: Atmospheres

Supporting Information for

A Schumann Resonance-based Quantity for Characterizing Day-to-day Changes in Global Lightning Activity

T. Bozóki[1,2], G. Sátori[1], E. Williams[3], A. Guha[4], Y. Liu[3], P. Steinbach[5,6], A. Leal[7,8], M. Atkinson[9], C. Beggan[10], E. DiGangi[11], A. Koloskov[12,13], A. Kulak[14], J. LaPierre[11], D.K. Milling[15], J. Mlynarczyk[14], A. Neska[16], A. Potapov[17], T. Raita[18], R. Rawat[19], R. Said[20], A.K. Sinha[21], Y. Yampolski[22]

[1]Institute of Earth Physics and Space Science (EPSS), Sopron, Hungary. [2]Department of Optics and Quantum Electronics, University of Szeged, Szeged, Hungary. [3]Parsons Laboratory, Massachusetts Institute of Technology, Cambridge, Massachusetts, USA. [4]Department of Physics, Tripura University, Agartala, India. [5]Department of Geophysics and Space Science, Eötvös Loránd University, Budapest, Hungary. [6]ELKH-ELTE Space Research Group, Budapest, Hungary. [7]Department of Physics and Langmuir Laboratory, New Mexico Institute of Mining and Technology, Socorro, NM, USA. [8]Graduate Program in Electrical Engineering, Federal University of Pará, Belem, Brazil. [9]HeartMath Institute, Boulder Creek, CA, USA. [10]British Geological Survey, Edinburgh, UK. [11]Advanced Environmental Monitoring (AEM), Maryland, USA. [12]Department of Physics, University of New Brunswick, Fredericton, NB, Canada. [13]State Institution National Antarctic Scientific Center of Ukraine, Kyiv, Ukraine. [14]Institute of Electronics, AGH University of Science and Technology, Krakow, Poland. [15]Department of Physics, University of Alberta, Edmonton, Canada. [16]Institute of Geophysics, Polish Academy of Sciences, Warsaw, Poland. [17]Institute of Solar-Terrestrial Physics SB RAS, Irkutsk, Russia. [18]Sodankylä Geophysical Observatory, University of Oulu, Sodankylä, Finland. [19]Indian Institute of Geomagnetism, Navi Mumbai, India. [20]Vaisala, Louisville, CO, USA. [21]Department of Physics, School of Science, University of Bahrain, Bahrain. [22]Institute of Radio Astronomy, National Academy of Sciences of Ukraine, Kharkiv, Ukraine.

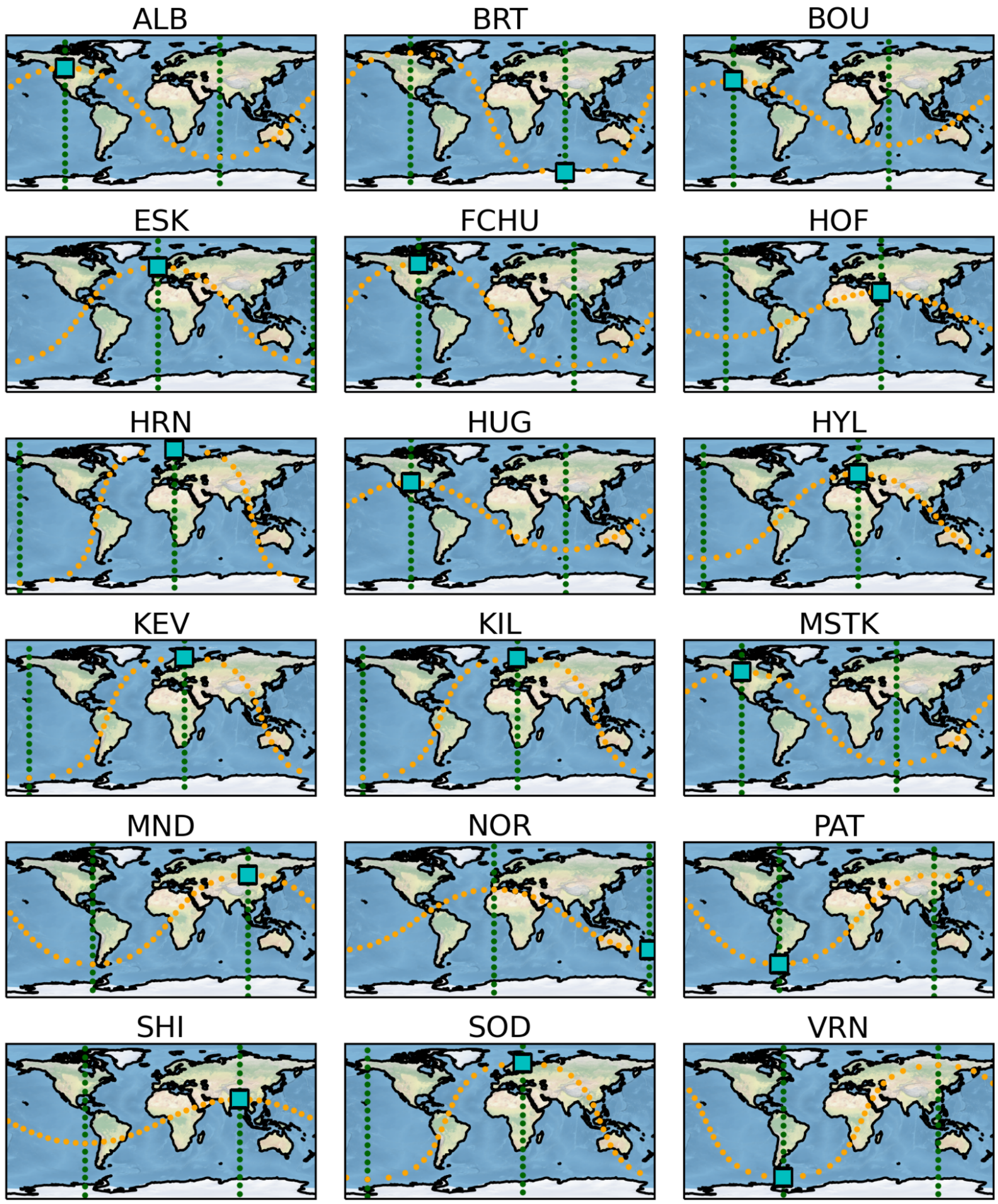

Figure S1 Propagation paths corresponding NS (orange) and EW (green) oriented induction coil magnetometers at the 18 SR stations used in the study (see Fig.1 and Table 1). In the chimney-by-chimney analyses (Fig.5 and Fig.6c,d) SR intensity records are averaged for the following stations and field components:

- Maritime Continent: BRT H_{EW}, ESK H_{NS}, FCHU H_{EW}, HOF H_{NS}, HRN H_{NS}, HUG H_{EW}, HUG H_{NS}, HYL H_{NS}, KEV H_{NS}, KIL H_{NS}, MND H_{EW}, MSTK H_{NS}, NOR H_{NS}, PAT H_{EW}, SHI H_{NS}, SOD H_{NS}, VRN H_{EW}
- Africa: ESK H_{EW}, HRN H_{EW}, HYL H_{EW}, KEV H_{EW}, KIL H_{EW}, MND H_{NS}, PAT H_{NS}, SHI H_{NS}, SOD H_{EW}, VRN H_{NS}, FCHU H_{NS}, HOF H_{NS}, HUG H_{NS}
- South America: HRN H_{NS}, HYL H_{NS}, KEV H_{NS}, KIL H_{NS}, MND H_{EW}, PAT H_{EW}, SHI H_{NS}, SOD H_{NS}, VRN H_{EW}.